UNIVERSIDADE DA BEIRA INTERIOR
Ciências

Mitochondrial genetic therapy in Parkinson's disease
Cloning mitochondrial gene ND1

Cátia Marlene do Carmo Baptista

Dissertação para obtenção do Grau de Mestre em
Biotecnologia
(2º ciclo de estudos)

Orientador: Prof.ª Doutora Diana Costa
Co-orientador: Prof.ª Doutora Fani Sousa

Covilhã, setembro de 2015

Aos meus queridos pais.

À melhor irmã do mundo e afilhado lindo.

Às minhas grandes amigas Sandra, Ana e Vanessa.

Acknowledgements

First of all, a big and sincere thanks to my supervisor Profª Diana Costa, PhD and co-supervisor Profª Fani Sousa, PhD for all the support and understanding throughout the development of this master's thesis.

I would like to thank Ruben Salvado for all explanations and tips that he gave me in the initial phase of the thesis.

To all Endocrinology group thank you for everything. To Eduarda Coutinho for her support and assistance throughout the development of the thesis. To Maria Inês Alvelos for the advices. To Joana Raimundo companionship. To Catarina Gonçalves for the friendship and support in difficult times.

To Patricia Pereira and Augusto Pedro for the tips regarding the growth and productivity studies and the tips in relation to *P.pastoris*. To Joana Valente for all the tips given throughout the thesis and the explanation and help in the purification step. To Carolina Costa for the company and help during the preparation of nanoparticles.

Also, I would like to thank João Matos and Engª Ana Paula for assistance in SEM sessions and to Carlos Gaspar for assistance in Zeta Sizer measurements.

Lastly, I'm very thankful to everyone that in a way or another contributed to the success of this thesis.

Thank you all so much,
Cátia Baptista

Resumo

A mitocôndria é um organelo celular que tem o seu próprio genoma, de cadeia dupla e circular que codifica 13 proteínas envolvidas no transporte de eletrões e fosforilação oxidativa. Estão presentes entre 10 e 100 cópias por célula somática e, dentro das células, as cópias de ADN mitocondrial (mtDNA) podem ser idênticas em sequência (homoplasmia) ou mtDNA "wild-type" e mutado podem existir em diferentes proporções (heteroplasmia). A heteroplasmia ocorre principalmente porque o mtDNA é particularmente suscetível a mutações, devido à sua proximidade a locais de geração de espécies reactivas de oxigénio.

Alterações no mtDNA podem provocar disfunções no mecanismo de fosforilação oxidativa, onde as exigências de ATP não são atingidas. O fenótipo da doença mitocondrial depende da heteroplasmia do mtDNA, quando é atingido um valor de mtDNA mutado entre 60-90%.

A ideia de que a disfunção mitocondrial poderia influenciar a doença de Parkinson surgiu com descoberta do mecanismo de ação do MPTP no início de 1980, que afeta o fluxo de eletrões no Complexo I. Diferentes mutações que afectam os genes que codificam as proteínas deste complexo têm sido associadas com a doença de Parkinson, duas delas sendo identificadas no gene mitocondrial ND1. Este facto faz com que o desenvolvimento de um vector com o gene mitocondrial ND1 seja uma abordagem muito interessante para aplicação na terapia génica mitocondrial (MGT) para o potencial tratamento da doença de Parkinson.

No presente trabalho foi desenvolvido um sistema para transportar um vector, desenhado no laboratório, com possível aplicação em terapia génica mitocondrial. O vector foi construído usando o plasmídeo pCAG-GFP e o gene mitocondrial ND1. Posteriormente, nanopartículas de $CaCO_3$ foram desenvolvidas para o seu transporte direccionado para a mitocôndria. O desenvolvimento deste projecto foi dividido em três etapas principais: i) construção do vector baseado na clonagem do gene mitocodrial ND1 no plasmídeo pCAG-GFP; ii) estudo de diferentes hospedeiros recombinantes para a amplificação do vector pCAG-GFP-mtND1; e iii) desenvolvimento de uma formulação adequada ao direccionamento do vector pCAG-GFP-mtND1 de forma eficiente para a mitocôndria.

O vector pCAG-GFP-mtND1 foi inserido em diferentes estirpes de *E. coli* e os estudos de crescimento foram muito semelhantes entre as estirpes transformadas, tendo sido observadas apenas algumas diferenças nos rendimentos específicos. Os sistemas de entrega preparados, demonstraram ser biocompatíveis, com eficiências de encapsulação acima de 50%, tamanhos inferiores a 280 nm e potenciais zeta positivos tornando-os adequados para MGT.

Palavras-chave

Mutações mitocondriais, doença de Parkinson, terapia génica mitocondrial, nanopartículas

Abstract

Mitochondria have their own genome, a circular double-stranded genome that encodes 13 proteins involved in electron transport and oxidative phosphorylation (OXPHOS). They are present in 10–100 copies per somatic cell and within the cell mitochondrial DNA (mtDNA) copies could be identical in sequence (homoplasmy) or wild-type and mutant mtDNA could exist in different ratios (heteroplasmy). Heteroplasmy occurs mainly because mtDNA is particularly susceptible to mutations due its proximity to reactive oxygen species (ROS) generation sites.

MtDNA dysfunction is characterized by a defective OXPHOS where ATP demands are not reached. The phenotype of the mitochondrial disease depends on the mtDNA heteroplasmy, when a threshold in the region of 60–90% mutated mtDNAs is reached.

The idea that mitochondrial dysfunction could influence Parkinson disease (PD) arose with the discovery of the mechanism of action of MPTP in the early 1980s that affected electron flow in Complex I (CI). Different CI related mutations have been associated with PD and two of them were identified in mtND1 gene. This fact makes the development of a mtND1 construct a very interesting approach for mitochondrial gene therapy (MGT) purposes in PD treatment.

Throughout this year, it was developed a nanocarrier to transport a designed vector with possible application in MGT. The vector was constructed using pCAG-GFP plasmid and the mitochondrial gene ND1 and $CaCO_3$ were developed for the directed transport of the plasmid towards mitochondria.

This research development was divided into three main stages: i) construction of a vector using an OXPHOS CI gene, mtND1 and the pCAG-GFP plasmid; ii) study of different recombinant hosts to produce the pCAG-GFP-mtND1 vector; and iii) development of a formulation for the efficient pDNA delivery into mitochondria.

The mtND1 construct was successfully obtained and inserted into different *E. coli* strains. The growth profiles were very similar between the strains, being observed sligth differences in the pDNA specific yields. The nanocarries obtained were biocompatible, displaying encapsulation efficiencies (EE) above 50%, sizes below 280 nm and positive zeta potential, making them very suitable for MGT.

Keywords

Mitochondrial mutations, Parkinson disease, mitochondrial gene therapy, nanoparticles

Index

Figures List

Tables List

Acronyms List

AD – Alzheimer disease

ADP - adenosine diphosphate

AIF - apoptosis-inducing factor

ALS - Amyotrophic lateral sclerosis

Apaf -1 - Apoptotic protease activating factor 1

APE1 - AP endonuclease-1

ATP - adenosine-5′-triphosphate

BER - Base excision repair

Ca^{2+} - Calcium

$CaCl_2$ - Calcium Chloride

$CaCO_3$ - Calcium Carbonate

CI – Complex I

DISC - death-inducing signaling complex

DNA - Deoxyribonucleic acid

DNA SSB - DNA single strand break

Dnm1l - dynamin-1-like protein

DOPE - Discrete Optimized Protein Energy

DQAsomes - DeQuAlinium-based liposome-like vesicles

DR - death receptor

dRp - DNA single strand break flanked by 3'-hydroxyl and a 5'-deoxyribosephosphate

EDTA - Ethylenediamine tetraacetic acid

EE - Encapsulation Efficiency

$FADH_2$ - Flavin Adenine Dinucleotide

FEN-1 - Flap endonuclease-1

Fis1 - fission protein 1

H_2O_2 - hydrogen peroxide

HD – Huntington disease

IMM - inner mitochondrial membrane

Kb - Kilobase

LB - Luria Broth

LP - Liposomes

LP-BER - Long pathway BER

Mfn - mitofusin

MGT - mitochondrial gene therapy

Mn - manganese

MnSOD - superoxide dismutase

MOMP - mitochondrial outer membrane permeabilization

mPTP - mitochondrial permeability transition pore

mtDNA - mitochondrial DNA

MTT - 3-(4,5-dimethylthiazol-2-yl)-2,5-diphenyltetrazolium bromide

NADH - nicotineamide-adenine-dinucleotide

$O2^{-\bullet}$ - superoxide anion

O_H - H-strand origin

$OH^{\bullet}$ - hydroxyl radical

O_L - L- strand origin

OM - outer membrane

OXPHOS - Oxidative phosphorylation

PCR - polymerase chain reaction

PD – Parkinson Disease

Pi - inorganic phosphate

PNA – peptide nucleic acid

Pol ß - polymerase ß

Q – Ubiquinone

R8 - octaarginine

RES - reticuloendothetial system

Rho_{123} - $Rhodamine_{123}$

RITOLS - RNA incorporation throughout the lagging strand

RNA - Ribonucleic acid

ROS - Reactive oxygen species

rRNA - Ribosomal RNA

SDS - *Sodium dodecyl sulfate*

SEM - Scanning Electron Microscopy

Smac - second mitochondria-derived activator of caspases

SP-BER - Short pathway BER

TAE - Tris-Acetate-EDTA

TB - Terrific Broth

TCA - tricarboxylic acid

TFN - tumor necrosis factor

TPP - triphenylphosphine

tRNA - Transfer RNA

YPD - Yeast extract peptone dextrose

ZFB – Zinc-finger binding proteins

Introduction

Human mitochondria are small cytoplasmic organelles, present in 10–100 copies per somatic cell (1). Mitochondria are different from other organelles with respect to their complex two membrane structure (2) and they contain a circular genome, mitochondrial DNA (mtDNA) that has been reduced during evolution through gene transfer to the nucleus (3). MtDNA encodes 13 polypeptides, 2 ribosomal RNAs and 22 RNA transcripts that contribute to 4 of the 5 respiratory chain complexes (1,4). By a process of oxidative phosphorylation (OXPHOS) mitochondria converts biochemical energy stored in food, through the oxidation of nutrients to produce adenosine-5′-triphosphate (ATP) (5).

MtDNA dysfunction is typically characterized by an inability to meet cellular ATP demand as a result of defective OXPHOS (4). Mitochondrial disease phenotype is dependent on mtDNA heteroplasmy, where disease manifests in cells carrying more than a certain threshold percentage of mutated mtDNA copies. Normally this threshold is in the region of 60–90% of mutated mtDNAs and changes between organs depending upon their energy requirements (1,6). It is described that 1 in 8000 individuals carry a mtDNA genetic disorder or are affected by a pathogenic mtDNA mutation (4).

Research undertaken to apply gene therapy for the treatment of mtDNA-related disorders is an emerging field known as mitochondrial gene therapy (MGT). Currently there are no recombinant human mtDNA constructs available for MGT (4) however cloning attempts of the human mtDNA were made in *S.cerevisiae* with success (1). Successful MGT has to follow three key conditions. First, the delivery of nucleic acids has to be made to the correct compartment, the mitochondria. Second, when applied to living cells, a beneficial effect on mitochondrial function should be obtained. Third, the modulation of mitochondrial function through MGT should occur *in vivo* and have a significant beneficial effect of the progress of the disease or disability (7).

Research in the field of nanotechnology has provided the development of systems that include nanovesicles and nanoparticles that have the potential of probing or manipulating mitochondrial function. Their affinity towards mitochondria comes from the presence of mitochondriotropic moieties, like rhodamine, methyl-TPP and dequalinium chloride, that reside in these novel carrier systems (DQAsomes, lipossomes, polymeric micelles, lipid based nanoparticles, quantum dots and MITO-porters) (8).

Nowadays, $CaCO_3$ based nanoparticles are extensively studied because of their many advantages such as biocompatibility, biodegradability, loading ability of different therapeutic agents, easy and cheap production and pH dependent dissolution. These nanoparticles are produced by co-precipitation of Ca^{2+} with nucleotides in the presence of CO_3^{2-}. This is an attractive option since it is a very simple technique, promotes gene delivery with protection of the encapsulated DNA from degradation and the nanoparticles can be internalized into different histological cell types (9 - 12). Natural compounds such alginate and cellulose were used in the

formulation of the $CaCO_3$ based nanoparticles to improve their stability and transfection efficiency and Rhodamine was used to direct the nanoparticles towards mitochondria (11-13).

1. Mitochondria

1.1. Structure and function

Mitochondria are small (0.5-1 μm) tubular-shaped cytoplasmic organelles present in 10–100 copies per somatic cell (1,14) Mitochondria are surrounded by two membranes, the outer membrane (OM), which is highly permeable, and the inner mitochondrial membrane (IMM) that restricts the entry of the polar molecules that lack their specific transporters (Figure 1). The inner membrane forms numerous folds (cristae), which extend into the mitochondrial matrix. Every one of these components have different roles, with the matrix and IMM representing the major working compartments of mitochondria (8,15).

Mitochondria plays a central role in growth, development and maintenance of vital processes. Their most crucial role is the generation of energy in the form of ATP through oxidative phosphorylation (OXPHOS) via the electron transport chain. Mitochondria are also involved in apoptosis, in dynamic movements (fusion/fission) required for correct respiratory activity and metabolic efficiency, regulation of intracellular calcium levels and generation of signaling molecules and toxic metabolites such as reactive oxygen species (ROS) (7,16,17).

Many studies recognize the importance of mitochondria in aging-related neurodegenerative diseases such as in Alzheimer's disease (AD), Parkinson's disease (PD), Huntington's disease (HD), and amyotrophic lateral sclerosis (ALS), which are associated with mitochondrial dysfunction (18).

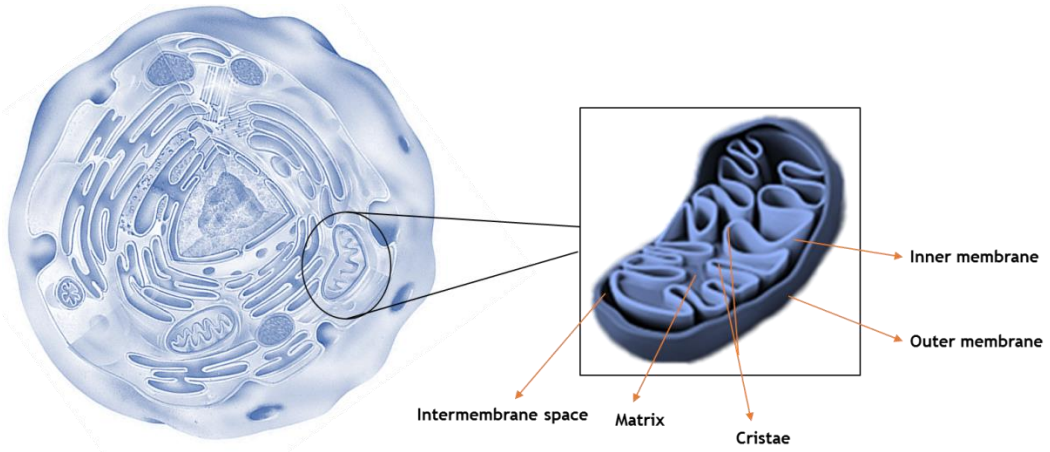

Figure 1- **Eukaryotic cell with a detailed mitochondria diagram showing the inner and outer membranes and the folded cristae.** Adapted from (15).

1.2. Mitochondrial DNA (mtDNA)

It is believed that mitochondria evolved from bacteria which developed a symbiotic relationship in which they lived inside larger cells (endosymbiosis) (15). As a legacy of their ancient endosymbiotic origin, the mitochondria retained their own diminutive genome of mitochondrial DNA although many of the genes essential for mitochondrial respiration have been translocated to the nuclear genome throughout the course of evolutionary history (5).

MtDNA is a circular double-stranded 16.569 Kb genome (Figure 2), encoding 13 proteins involved in electron transport and oxidative phosphorylation. The subunit proteins of respiratory complexes I, III, IV and V are encoded by mtDNA whereas protein subunit of complex II is solely encoded by nuclear genes (8). In addition, human mitochondrial DNA encodes 2 rRNA (16S and 12S rRNA) and 22 tRNAs, which are required for translation of the proteins encoded by the organelle genome. Only 6% of the mtDNA is noncoding, mainly located in the D-loop, and is involved in the replication and transcription of the mtDNA (15,19).

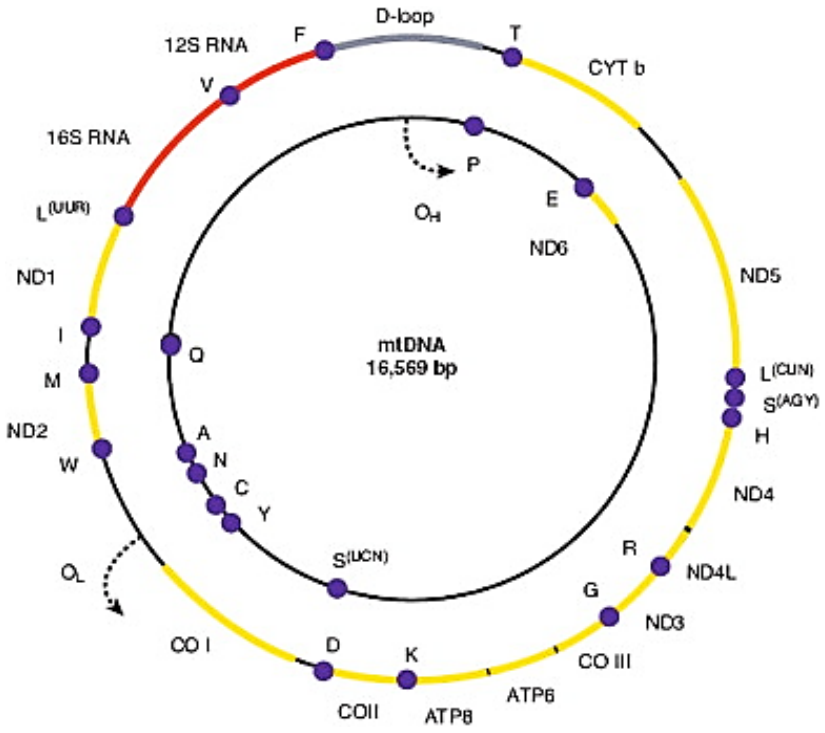

Figure 2 - **Human mtDNA.** Yellow: Protein coding genes; Red: rRNA; Purple: tRNA; Origins of replication: O_H for the H-strand origin and O_L for the L- strand origin. Adapted from (14)

The genetic code of animal and fungal mitochondria differs from the standard code used in all prokaryotic and eukaryotic nuclear genes. It differs as well from specie to specie (Table 1) (20).

Table 1 - **Genetic Code in Mitochondria.** Adapted from (20)

	Mitochondria					
Codon	**Standard Code: Nuclear-Encoded Proteins**	**Mammals**	***Drosophila***	***Neurospora***	**Yeasts**	**Plants**
UGA	Stop	Trp	Trp	Trp	Trp	Stop
AGA, AGG	Arg	Stop	Ser	Arg	Arg	Arg
AUA	Ile	Met	Met	Ile	Met	Ile
AUU	Ile	Met	Met	Met	Met	Ile
CUU, CUC, CUA, CUG	Leu	Leu	Leu	Leu	Thr	Leu

1.2.1. MtDNA Replication

MtDNA replication is not controlled by the cell cycle and is continuously recycled (21). Currently, the mechanism is unclear and three models are suggested, which are known as Strand-Displacement, Strand-Coupled and RITOLS models and are represented in figure 3 (22).

The Strand-Displacement model was elaborated in the early 1970s. In this model mtDNA is replicated in an asymmetric way. First DNA synthesis is primed and replication through the O_H strand within the D-loop occurs. After two-thirds of the emerging H strand was replicated, the O_L strand is exposed and initiation of emerging L strand synthesis is allowed (23).

The Strand-Coupled model describes that beyond the D-loop is a region of replication initiation. In that region, both strands are synthesized in both directions as the conventional double-stranded replication forks extent through continuous synthesis of leading and discontinuous synthesis of lagging strands (24).

The RITOLS model is based on the observation of RNA incorporation throughout the lagging strand. Replication initiates at O_H and DNA synthesis progresses with parallel incorporation of RNA on the lagging strand. At some point in O_L, DNA synthesis initiates and the lagging strand RNA is replaced by, or converted to, DNA (25).

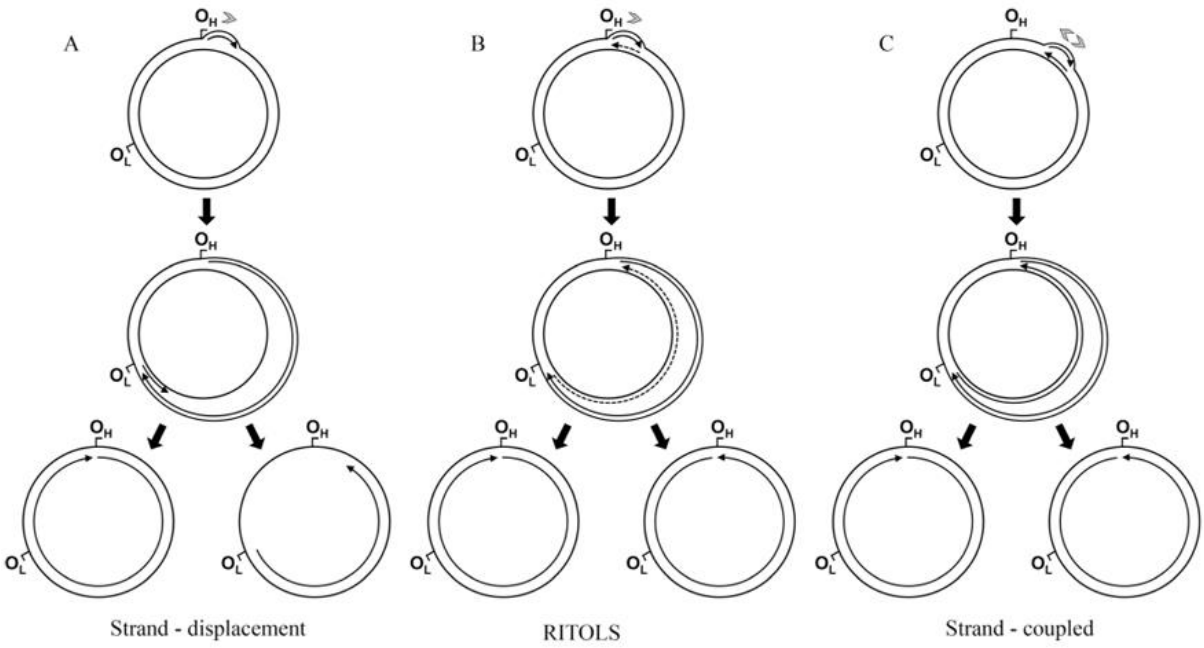

Figure 3 – **Proposed models of mammalian mtDNA replication.** Adapted from (26).

1.2.2. MtDNA mutations and repair mechanisms

MtDNA is constantly exposed to harmful agents. Therefore, many lesions can occur in mtDNA. The most studied of them all is the oxidative damage because mitochondria are the major cellular source of ROS (27).

DNA repair pathways are employed depending on the type of DNA damage that needs to be repaired. Base excision repair (BER) is a pathway that repairs simple lesions such as alkylation or oxidation products caused by ROS. There are two major BER sub-pathways in mammalian cells, the long patch BER (LP-BER) and the short patch BER (SP-BER) (figure 4). In the SP-BER a DNA glycosylase initiates the process by removing the damaged base. AP endonuclease-1 (APE1) cuts the phosphodiester backbone and a dRp (DNA single strand break flanked by 3'-hydroxyl and a 5'-deoxyribosephosphate) is formed. Pol ß cleaves the 5'-dRP moiety and at the same time adds a single correct nucleotide into the one-nucleotide gap. Lastly, the DNA single strand break (DNA SSB) ends are sealed by the XRCC1-Lig IIIα complex. LP-BER occurs when the 5'-dRP moiety is resistant to cleavage by Pol ß. A polymerase switch occurs and Pol δ/ε is recruited adding into the repair gap 2 to 8 correct nucleotides. Pol δ/ε activity creates a 5'-flap structure that is excised by FEN-1 and afterwards the remaining DNA SSB ends are then sealed by Lig I (28,29).

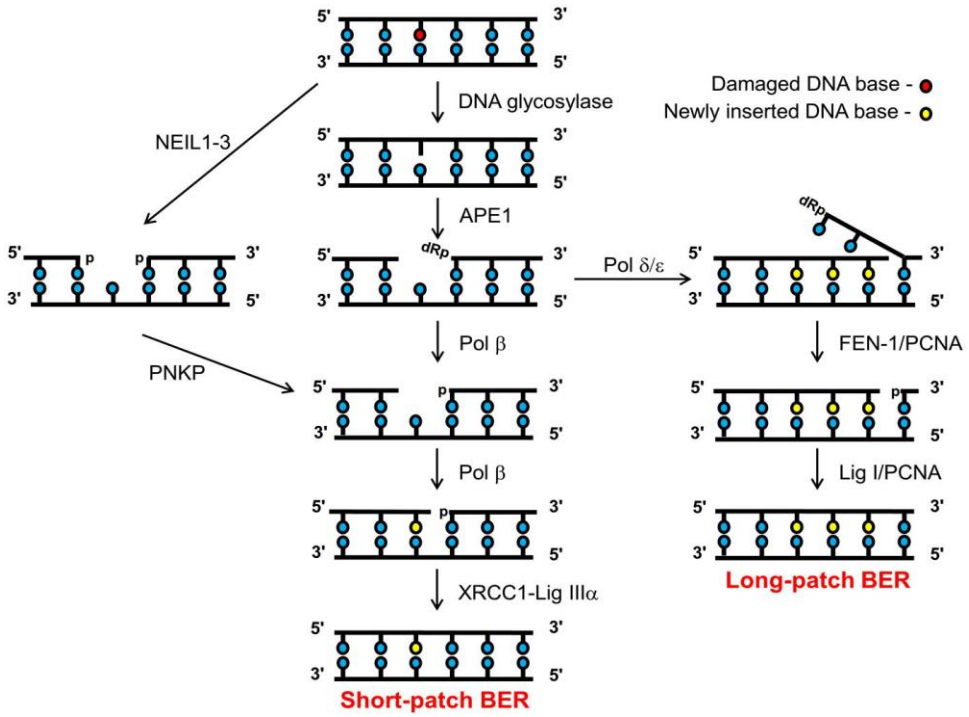

Figure 4 - **Base excision repair pathways.** Adapted from (29).

1.2.3. Heteroplasmy and threshold effect

Within a single cell or tissue all mtDNA copies could be identical in sequence (homoplasmy) or wild-type and mutant mtDNA could exist in different ratios (heteroplasmy). The ratio of wild-type to mutant mtDNA determines the onset of clinical symptoms and a minimum proportion of mutated mtDNA is necessary before biochemical defects and tissue dysfunction become apparent. This is called threshold effect and varies for each mutation and differs amongst tissues, being lower in tissues highly dependent on OXPHOS metabolism such as brain, heart and skeletal muscle. Usually, clinical manifestations occur when the threshold value is between 60% to 90% of mutant to wild-type mtDNA (1,6,30,31) The study of threshold effect in diseases was possible due to the creation of cybrids, cells lacking mtDNA where were introduced mitochondria from cells obtained from patients. Cybrids containing different proportions of mutated mtDNA from 0 to 100% permitted to study the effects of a certain mutant load on the activity of respiratory chain complexes, mitochondrial respiration and cell growth (32).

A powerful tool to treat mitochondrial diseases would be the ability to manipulate mtDNA heteroplasmy and various studies were already made in this field (figure 5). Dai and co-workers studied the effect of rapamycin, an anti-cancer drug, in enhancing mitophagy to select mostly dysfunctional mitochondria with higher levels of mutations, which resulted in decreasing mutation levels over time in a human cybrib expressing a heteroplasmic mtDNA G11778A mutation (33). Also Tanaka and co-workers studied the removal of pathogenic mtDNA by

targeting restriction endonucleases to mitochondria of heteroplasmic cells, eliminating with success a mutant mtDNA with the Mt8993T>G mutation from cultured cybrids (34). Minczuk and co-workers demonstrated that it is possible to target and alter mtDNA in a sequence-specific manner by using zinc finger technology (35). Moreover, the use of peptide nucleic acid (PNA) oligomers that could bind selectively to complementary mtDNA inhibiting replication and translation was studied by Muratovska and co-workers (36).

Other methodologies like using endurance and resistance exercises shown to be safe and effective in inducing increase of wild-type mtDNA levels in muscles (37).

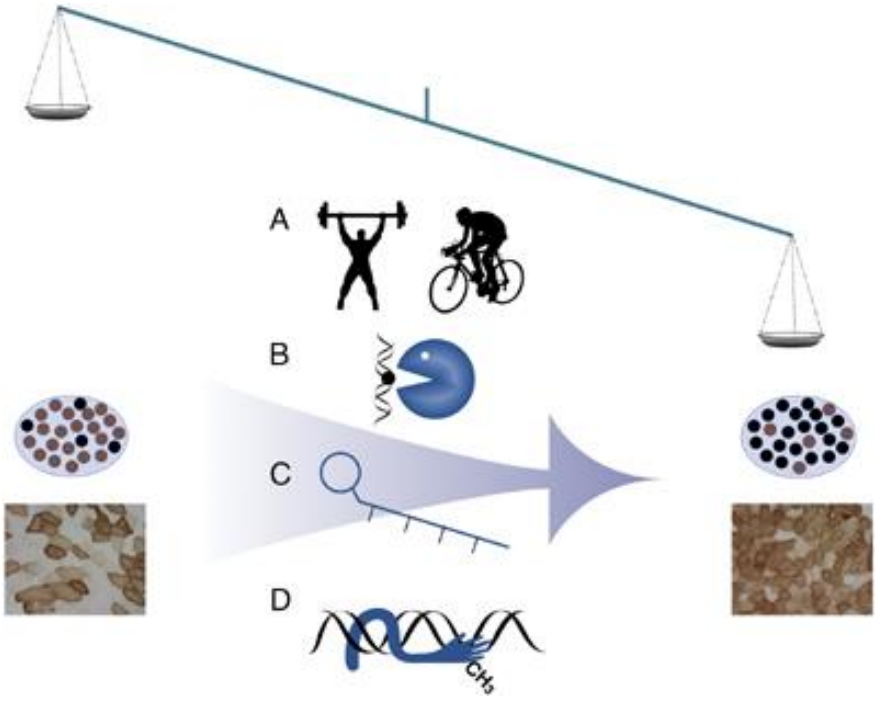

Figure 5 **- Manipulation of mtDNA heteroplasmy.** Heteroplasmic mitochondria containing both wild type (brown) and pathogenic (black) mtDNA are presented in the figure. Strategies to manipulate mtDNA heteroplasmy: A) Endurance or resistance training; B) Targeting restriction endonucleases to mitochondria; C) peptide nucleic acid (PNA) oligomers; D) Zinc-finger binding proteins (ZFB) that could methylate a specific mtDNA mutation. Adapted from (38).

1.2.4. Inheritance of mtDNA

Although nuclear genes display Mendelian segregation, mtDNA is inherited in a non-Mendelian manner. MtDNA is inherited from the mitochondria in the oocyte and this inheritance is generally referred to as "maternal inheritance of mtDNA" (39). MtDNA from sperm is removed by ubiquitination during mammalian zygote formation. Up till now only a single case of paternal transmission in humans has been recorded (21).

MtDNA mutation is believed to occur either in the female germ line or early in embryonic development but, unexpectedly, only a few mutations are transmitted to each successive generation (40). The mitochondrial genetic bottleneck theory states that, before

oogenesis, a size decrease occurs in the population of maternal mtDNA molecules, causing a genetic bottleneck where randomly different mtDNA are segregated. The random segregation of wild type and mutant mtDNAs creates different levels of heteroplasmy (figure 6) (41).

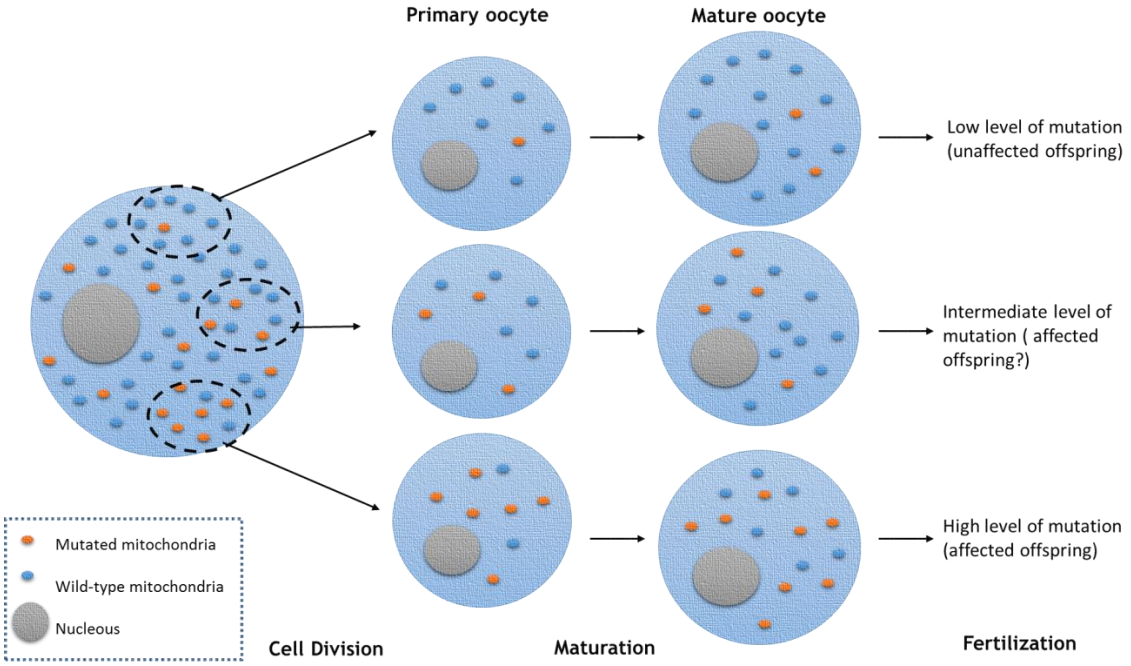

Figure 6 - **Mitochondrial genetic bottleneck theory.** Mitochondria are randomly segregated through cell division to the primary oocytes. Then, depending on the amount of mutated mithocondria acquired, mature oocytes could have different levels of mutation. Adapted from (69).

1.3. Role of mitochondria in the living cell

1.3.1. Electron transfer system and ATP synthesis

By a process of oxidative phosphorylation (OXPHOS) mitochondria converts biochemical energy stored in food, through the oxidation of nutrients to produce adenosine-5′-triphosphate (ATP) (5). OXPHOS is a result of the mitochondrial respiratory chain that has four multisubunit polypeptide complexes located in the IMM (Figure 7). This polypeptide complexes are NADH-Q oxidoreductase, succinate-Q reductase, Q-cytochrome c oxidoreductase, and cytochrome c oxidase also designated by Complex I, II, III, and IV, respectively.

Electrons are transferred from NADH to O_2 in chain by the three large protein complexes (I, III and IV). The electron flow within these transmembrane subunits leads to the transport of protons across the IMM. Ubiquinone (Q) carries electrons from NADH-Q oxidoreductase to Q-cytochrome c oxidoreductase and electrons from $FADH_2$ (generated in the citric acid cycle) to Q-cytochrome c oxidoreductase (generated through succinate-Q reductase). Cytochrome c shuttles electrons from Q-cytochrome c oxidoreductase to cytochrome c oxidase.

The electrochemical gradient generated across the IMM is then used by ATP synthase to catalyze the conversion of adenosine diphosphate (ADP) and inorganic phosphate (Pi) to ATP(14)(42).

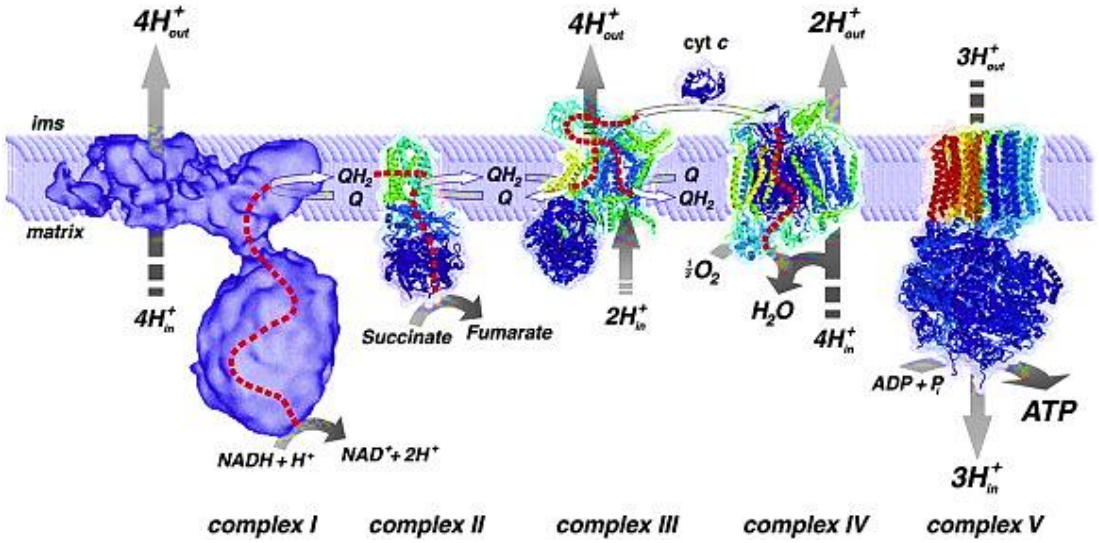

Figure 7 - **Mitochondrial respiratory chain.** Adapted from (14).

1.3.2. Production of Reactive oxygen species (ROS)

Redox-dependent processes influence many cellular functions, as differentiation, proliferation, and apoptosis. Mitochondria has a great role in this processes, because generates ROS and respond to ROS-mediated changes in the cellular redox state (43).

ROS generation occurs within complex I and III of mitochondrial respiratory chain. When oxygen is reduced by one electron (e-), superoxide anion ($O2^{\bullet -}$) is formed. Superoxide is a short-lived free radical that reacts rapidly with a wide range of chemical substrates, including itself. Superoxide engages spontaneously in dismutation, catalyzed by superoxide dismutase. Dismutation of $O2^{\bullet -}$ produces hydrogen peroxide (H_2O_2), posteriorly reduced to water or to hydroxyl radical ($OH^{\bullet}$). $OH^{\bullet}$ formation is catalysed by reduced transition metals, which in turn may be re-reduced by $O2^{\bullet -}$ propagating this process. Also, $O2^{\bullet -}$ may react with other radicals like nitric oxide ($NO^{\bullet}$) which product is peroxynitrite (ONOO−), a very powerful oxidant. The oxidants derived from $NO^{\bullet}$ are called reactive nitrogen species (RNS) (44,45).

Excess of ROS production causes damage in key components of cells like lipids, proteins and nucleic acids, the former including production of thymine dimers (figure 8). Due to the mutagenic nature of many of the ROS-induced lesions, mitochondrial free radicals are thought to be an important source of mtDNA mutations and DNA instability (3,28,45).

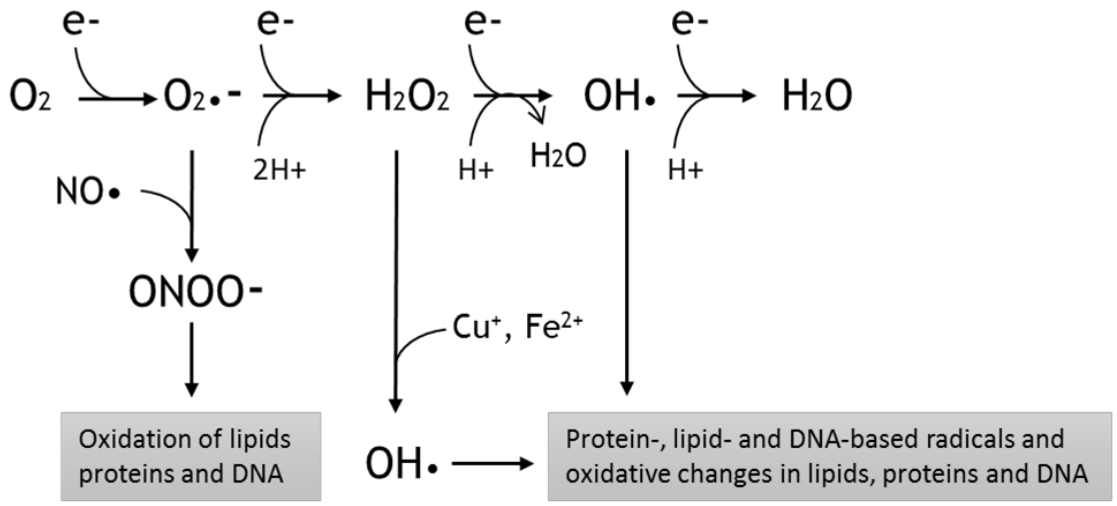

Figure 8 - **Effects of reactive oxygen species.**

1.3.3. Ca^{2+} homeostasis

Mitochondria's capacity to accumulate Ca^{2+} was described in the 1960's (46,47). Calcium is an important regulator of mitochondrial function (figure 9) and stimulates ATP synthesis. Dysregulation of mitochondrial Ca^{2+} homeostasis is recognized to play a key role in several pathologies (46,48,49). Matrix Ca^{2+} is a positive allosteric regulator of dehydrogenases in the tricarboxylic acid (TCA) cycle and influences the activity of the electron transport chain complexes. When the mitochondrial Ca^{2+} concentration rises, ATP production increases however, an overload of Ca^{2+} can induce the opening of the mitochondrial permeability transition pore (mPTP) in the inner mitochondrial membrane (IMM). This phenomenon changes the mitochondrial membrane potential and caspase cofactors are released into the cytoplasm triggering an apoptotic cascade (46,50).

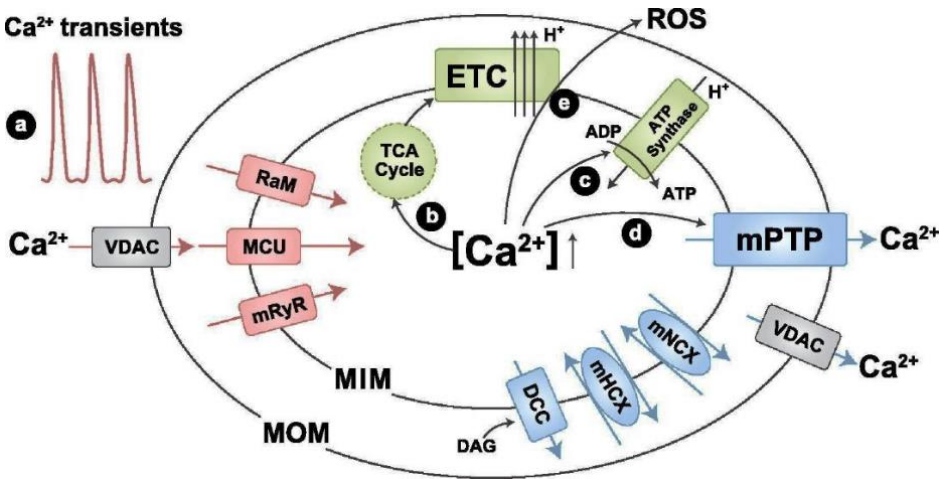

Figure 9 - **Mitochondrial Ca^{2+} channels/transporters**. The role of Ca^{2+} in mitochondrial function is also showed. Adapted from (51).

1.3.4. Programmed Cell Death (PCD)

Apoptosis is essential in tissue homeostasis. It has two main pathways, the extrinsic and the intrinsic apoptosis (figure 10) (52).

The extrinsic pathway involves signaling through cell surface receptors of the tumor necrosis factor (TNF) receptor family. These receptors have an intracellular protein domain called death receptor (DR). The ligand-induced activation of DR causes the formation of the death-inducing signaling complex (DISC) by recruiting procaspase-8. Procaspase-8 is cleaved and the mature protease (caspase 8) activates caspase-3 leading to cell death (53-56).

The Intrinsic pathway is the mitochondrial pathway of apoptosis. It is activated as a response to stress conditions, like DNA damage or oxidative stress, resulting in mitochondrial outer membrane permeabilization (MOMP) (54). Pro-apoptotic Bcl-2 family regulate MOMP by forming external membrane pores (57) leading to the release of mitochondrial intermembrane proteins as cytochrome c and second mitochondria-derived activator of caspases (Smac) into the cytosol (58). Cytochrome c forms a protein complex composed of cytochrome c, Apaf-1 and caspase-9, activating caspase-9 that subsequently activates caspase-3 leading to apoptosis (56).

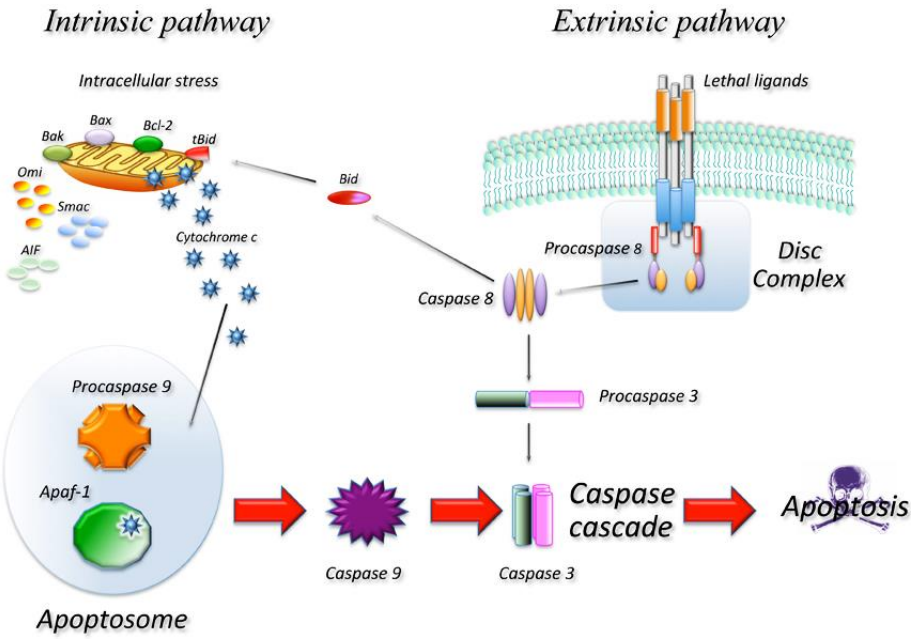

Figure 10 - **Molecular pathways that lead to apoptosis. Extrinsic pathway:** A lethal ligand triggers DR leading consequently to caspase 8 activation by DISC complex. Caspase 8 stimulates caspase 3 leading to apoptosis and Bid leading to MOMP. **Intrinsic pathway:** Intracellular stress induces MOMP, regulated by Bcl-2 family. MOMP causes the externalization of Cytochrome c forming a protein complex (Apoptosome) with Apaf-1 and procaspase 9. Therefore caspase 9 is activated leading to caspase 3 activation and apoptosis. AIF (apoptosis-inducing factor), Smac and Omi are also released from mitochondria. Adapted from (54).

1.3.5. Mitochondrial dynamics: Fission and Fusion

Mitochondria's shape is very dynamic. Under respiratory conditions mitochondria undergo frequent cycles of fusion and fission to allow spreading of metabolites and macromolecules throughout the entire compartment (59).

In mitochondrial fusion the four lipid bilayers are merged together. It requires two isoforms of mitofusin1 (Mfn1) and mitofusin2 (Mfn2), which are both anchored to the OMM. They have two transmembrane domains, a cytosolic N-terminal GTPase domain and two cytosolic hydrophobic coiled-coil domains. The coiled-coil domains of Mfn1 and Mfn2 help in binding adjacent mitochondria in both homo-oligomeric and hetero-oligomeric manner. Fusion-deficient cells have greatly diminished respiratory capacity and reduced cell growth.

Mitochondrial fission occurs by interaction of two proteins: dynamin-1-like protein (Dnm1l) and fission protein 1 (Fis1). With the help of Fis1, Dnm1l (localized in the cytosol) is recruited to the constriction sites of the membrane. Once inside, Dnm1l oligomerizes into a ring around the mitochondria. The self-assembly of DLP1 stimulates the final step of fission (60,61).

Cycles of fusion and fission (Figure 11) occur for mitochondria to adapt to the energetic requirements of the cell. The fusion is preferred when optimal mitochondrial function is needed, and the fission is required for elimination of damaged and inactive organelles by autophagy (59).

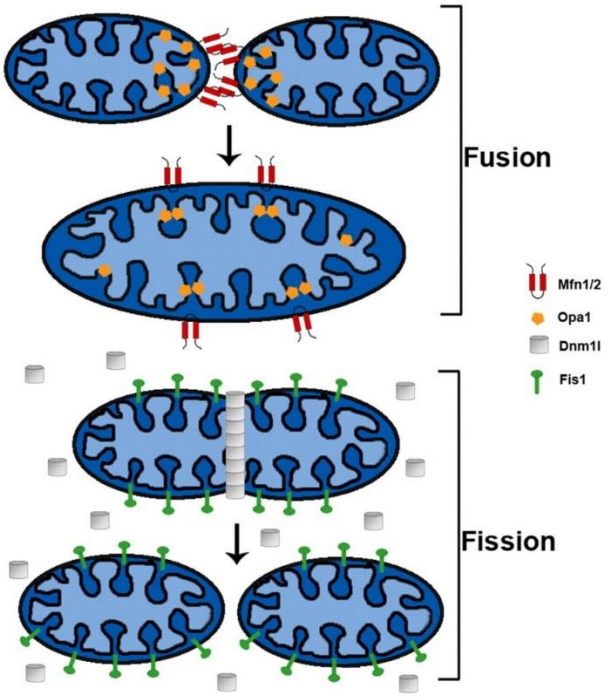

Figure 11 - **Schematic representation of mitochondrial fusion and fission events.** Adapted from (61).

2. Mitochondrial diseases

Mitochondria are associated with many human inherited disorders and diseases, such as neurodegenerative disorders, cardiomyopathies, metabolic syndrome, cancer, and obesity. Mitochondrial diseases can affect any organ system, manifest at any age, and can be inherited from an autosome, an X chromosome, or maternally. Reports indicate that 1 in 8000 individuals carry an mtDNA genetic disorder or are affected by a pathogenic mtDNA mutation and currently there is no cure for mitochondrial disorders and the existing treatments are directed to the relief of the symptoms (3,4).

The principal function of mitochondria is ATP production through OXPHOS and apart from energy conversion, mitochondria take part in a number of other processes, as previously mentioned. Mitochondrial diseases occur mostly when one or more of the OXPHOS complexes are dysfunctional, where this dysfunction together with other factors promotes a vicious cycle (figure 12) (62).

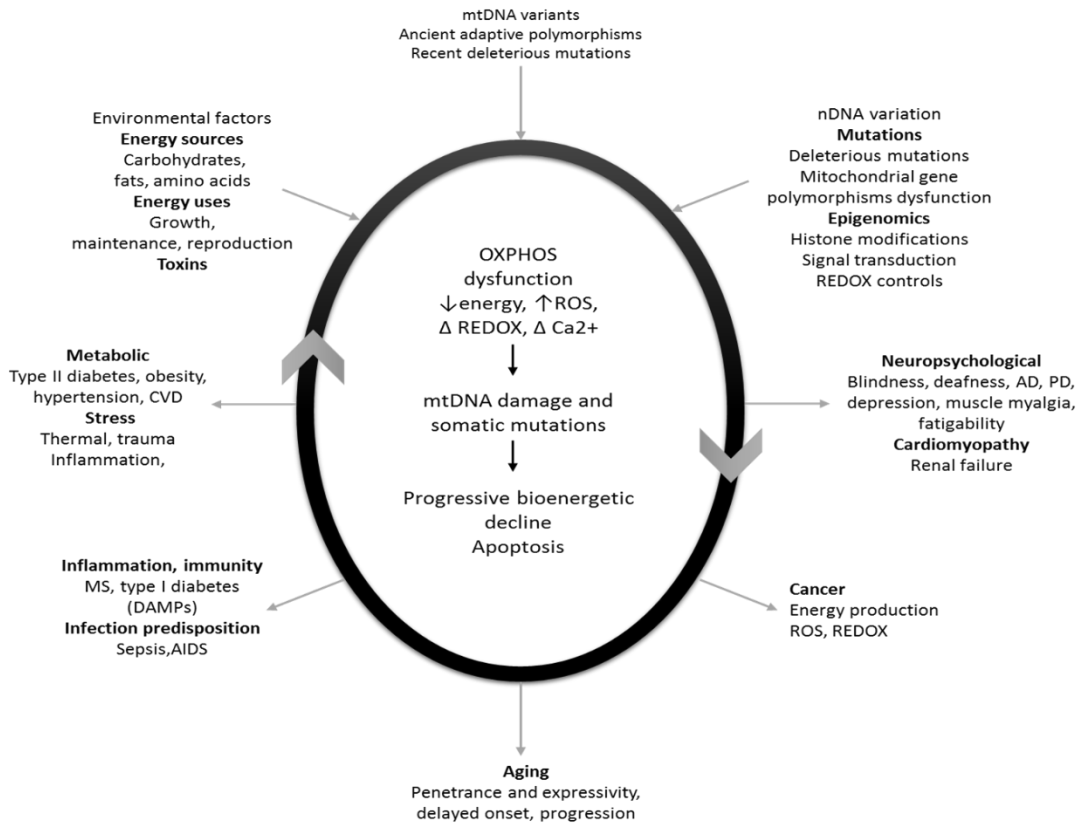

Figure 12 - **Mitochondrial etiology of complex disease.** Adapted from (63).

2.1. Cytopathies and mutations

Mitochondrial pathologies (figure 13) present a heterogeneous group of multisystem disorders characterized by abnormalities of the mitochondrial ultrastructure as well as of

oxidative phosphorylation functioning. Defects in OXPHOS affect any tissue leading to the concept of mitochondrial cytopathies, which preferentially affect the muscle and nervous systems. They are caused either by mutations in the maternally inherited mitochondrial genome or by nuclear DNA mutations (4,64,65)

Mitochondrial genome is particularly vulnerable to mutations because of its proximity to ROS generation sites and it is not protected by histones or membranes (66). Currently, more than 250 pathogenic mtDNA mutations have been described (67) and the phenotype of the disease depends on the mtDNA heteroplasmy and on its threshold percentage on the cells (60 – 90% mutated mtDNAs) (1,6).

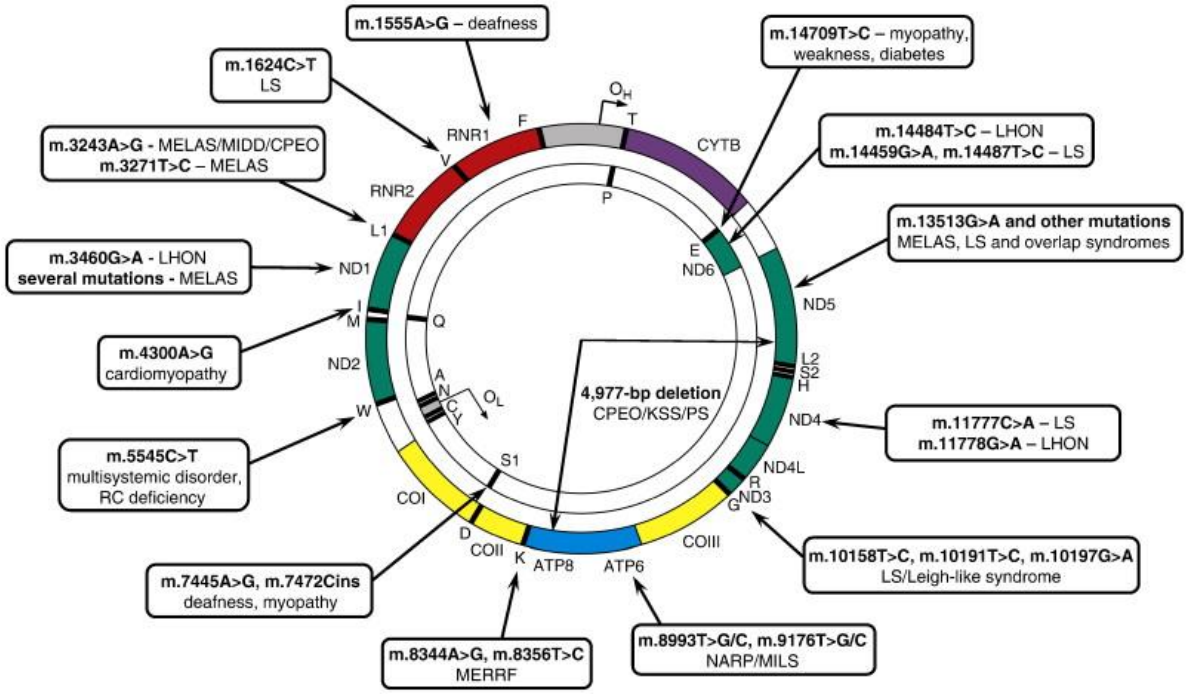

Figure 13 **- MtDNA mutations and corresponding diseases.** Adapted from (31).

2.2. Aging

The involvement of mtDNA in the aging process is mostly because of its proximity to the mitochondrial respiratory chain, source of ROS generation. ROS create an environment in which spontaneous mtDNA mutations are more possible to occur (28,68).This results in an exponential rise in oxidative damage, where cellular and tissue functions are loss with a combination of energy insufficiency, signaling defects, apoptosis, and replicative senescence. An increased number of COX-deficient cells and higher levels of mutated mtDNA is observed within the process (69).

2.3. Neurodegenerative diseases: Parkinson (PD)

Neurodegenerative diseases are characterized by the progressive loss of neurons and result in memory loss, movement problems, cognitive deficits, emotional alterations and behavioral problems. Environmental factors, genetic mutations and old age, are the major risk factors. Disease-linked mutations in genes provide key clues to the molecular mechanisms involved in the pathology and have been studied intensively over the last decades (61,70).

Parkinson (PD) is a neurodegenerative disease associated with progressive resting tremor, rigidity, bradykinesia, gait disturbance, postural instability and dementia where degeneration of dopamine neurons in the substantia nigra occurs (61,71). It is one of the most-common neurological disorders, affecting about 1-2% of the population over age of 60 years (72). PD movement symptoms are caused by the loss of inhibitory dopamine neurons which causes an increase in the activity of the subthalamic nucleus and the globus pallidus. The formation of Lewy bodies is a second neuropathological trait of PD where these cellular inclusions contain a dense core of filamentous material surrounded by a halo of fibrils comprising mainly α-synuclein (61). The accumulation of α-synuclein contributes to mitochondrial fragmentation and also damages the function of Complex I (CI) (73). In PD patients, deficits in CI activity were detected in the striatum, cortical brain tissue, fibroblasts, blood platelets with a slight variability in skeletal muscle and lymphocytes (74). A few genes associated with Mendelian forms of PD such as autosomal dominant (SNCA, LRRK2) or recessive (PARK2/Parkin, PINK1, DJ-1, ATP13A2) inheritance have been discovered throughout the past fifteen years (75).

The idea that mitochondrial dysfunction could influence PD disease emerged with the discover of the mechanism of action of MPTP in the early 1980s where a Parkinson's-like syndrome was caused by MPP^+ blockage of electron flow in CI (44,76). The reduced CI activity was also observed in cybrids with mtDNA from PD patients, demonstrating that mtDNA mutations may have influence in a few patients with PD. The cybrids gained features from the PD patients which showed reduced mitochondrial membrane potential, mitochondrial respiration, impaired mitochondrial biogenesis and abnormal Ca^{2+} handling (70).

Genetic evidences suggest that, besides the mitochondrial CI defect, mutations in mtDNA and mitochondrial dysfunction, including defects in bioenergetics, mitochondrial fusion/fission, mitochondrial movement, and transcription play a role in the pathogenesis of PD (70). Furthermore, diverse CI mutations have been associated with PD (77). Two different mutations in mtND1 gene were identified (table 2) making the development of an mtND1 construct a very interesting approach for gene therapy purposes in PD treatment.

Table 2 - **Confirmed mtDNA variations associated with PD disease.** Adapted from (78).

Variation	*mtDNA gene*
A3397G	ND1
T4216C	ND1
T4336C	tRNA(Gln)
A4336G	tRNA(Gln)
A4917G	ND2
G5460A	ND2
G9055A	ATP6
G10398A	ND3
A11084G	ND4
G13708A	ND5
G15928A	tRNA(Thr)
G15950A	tRNA(Thr)
T15965C	tRNA(Pro)

2.4. Diagnosis of mtDNA disease

The diagnosis is very complex when it comes to mitochondrial diseases. It is difficult due to the mtDNA heteroplasmy and lack of a clear genotype, phenotype correlations and the complex interactions between the nuclear and mitochondrial genome. Laboratory diagnosis of mtDNA disease often involves to gather many types of information from clinical to histochemical, biochemical and genetic allowing the development of rational diagnostic algorithms (figure 14) (31).

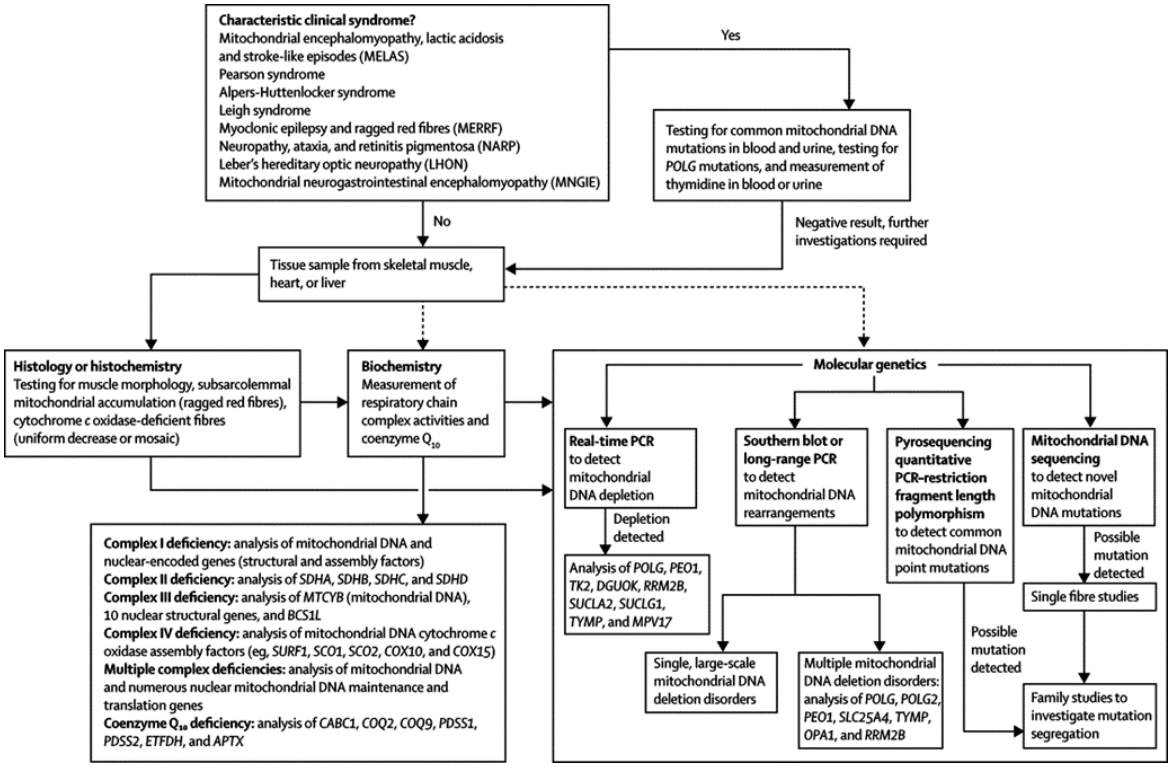

Figure 14 - **Algorithm for investigation of mitochondrial disease.** Adapted from (69).

No specific pharmaceutical drugs show to treat mitochondrial disease effectively in large-scale clinical trials (69). In this sense, both new therapies and approaches need to be developed in order to evolve in the treatment of patients suffering from mitochondrial disorders. Gene therapy for treatment of these diseases offers an interesting alternative to the therapeutic strategies that are currently applied (4).

3. Gene Therapy: Mitochondrial gene therapy (MGT)

The growing interest in gene therapy has become a strong incentive to develop gene vectors with high transfection efficiency and minimized toxicity. Although viral vectors demonstrated more effectiveness, disavantages like toxicity and production difficulties limited their applications. Consequently non-viral vectors are prefered because of their lower immune response and higher safety although transfection efficiency is reduced (80).

Genetic manipulation of mtDNA and its gene products is an important subject for investigation regarding the mtDNA disorders treatment. One important aim should be the correction of OXPHOS's defects as it is a common feature among mtDNA disorders. Research in gene therapy for mtDNA disorders treatment is an emerging field known as mitochondrial gene therapy (MGT). Currently there are no recombinant human mtDNA constructs available for MGT (4) however successful cloning attempts of the human mtDNA where made in *S.cerevisiae* (1).

Importation of wild-type copies or relevant sections of DNA or RNA into mitochondria, manipulation of mitochondrial genetic content or rescue of a defect by expressing an

engineered product from the nucleus are different approaches that could be taken in MGT (81). For this to occur, biological barriers should be surpassed by using different strategies (figure 15).

To be successful MGT has to follow three key conditions. First, the delivery of nucleic acids has to be made in the correct compartment of mitochondria. Second, when applied to living cells, a beneficial effect on mitochondrial function should be obtained. Third, the modulation of mitochondrial function through MGT should occur *in vivo* and have a significant beneficial effect of the progress of the disease or disability (7).

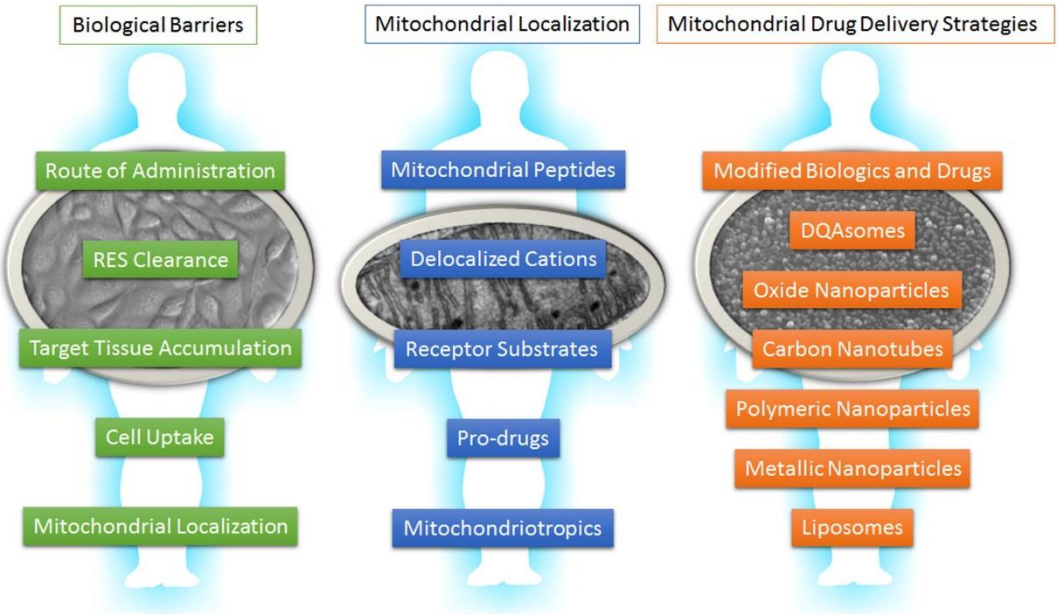

Figure 15 - **Delivery of therapeutic agents into Mitochondria.** The delivery only is achieved when biological barriers are surpassed and the therapeutic agent reaches mitochondria. Several strategies can help to overcome biological barriers avoiding RES (reticuloendothetial system) clearance and enabling target site accumulation. When reaching the cell, mitochondrial localization can be achieved by exploiting the negative membrane potential of mitochondria and targeting mitochondrial receptors with peptides and substrates, or using pro-drugs and characterized mitochondriotropics. Adapted from (82).

3.1. Construction/amplification of a recombinant human mtDNA construct for MGT

MGT is an emerging field for mitochondrial diseases treatment. When one or more specific genes are identified as the major responsible for a disease they can be used in gene therapy for the treatment of that disease. In this work mtDNA was extracted from human blood and an OXPHOS complex I gene, mtND1, was amplified by polymerase chain reaction (PCR) with specific primers. The plasmid selected was pCAG-GFP that produces the green fluorescent protein when present in the cytoplasm of cells, thus allowing to conclude about the construct presence by confocal microscopy.

The enzymatic digestion with the same enzymes in both mtND1 and in pCAG-GFP allowed the desired construct to be obtained by a binding reaction. The amplification of the construct was made by transforming competent *E.coli* cells. When purified, the construct can be used for the formulation of nanoparticles with specific mitochondriotropic moieties that direct the nanoparticle to mitochondria.

3.2. Nanotechnology

Nanobiotechnology applies principles and techniques at a nanoscale level to comprehend and change biosystems by using biological principles and materials to create new devices and systems (83). In the last decade the increase of therapeutic approaches targeting mitochondria, such as MGT, has resulted in the necessity to create novel delivery systems that have a selective delivery of nucleic acids into mitochondria. Liposomes, DQAsomes, polymeric micelles and lipid based nanoparticles (figure 16) associated with diverse mitochondriotropic moieties as rhodamine and triphenylphosphine (TPP), are examples of new non-viral delivery systems that arouse to fulfill this necessity (8).

Liposomes (LP) are generally biocompatible and non-toxic thus having a great potential for gene delivery. Its surface can be easily modified with mitochondriotropic ligands to target mitochondria and deliver the therapeutic agent. Examples of liposomal systems for delivery to mitochondria include octaarginine (R8) - modified liposomes, cell-targeting liposomes equipped with pH-dependent fusogenic peptides such as GALA and incorporation of (TPP) to the liposomal bilayer (8,28)

DQAsomes are liposome-like cationic vesicles derived from the amphiphile dequalinium. These mitochondriotropic vesicles are capable of condensing pDNA and form DQAsome-pDNA complexes protecting the pDNA from nucleases and localizing mitochondria in living cells (12,84,85).

MITO-Porters are liposome-based nanocarriers that deliver the desired nucleic acids to mitochondria via a membrane-fusion mechanism. This device includes ligands for specific receptors, pH-sensitive fusogenic peptides (DOPE) for endosomal escape and mitochondriotropic residues for enhanced mitochondrial delivery (8,86).

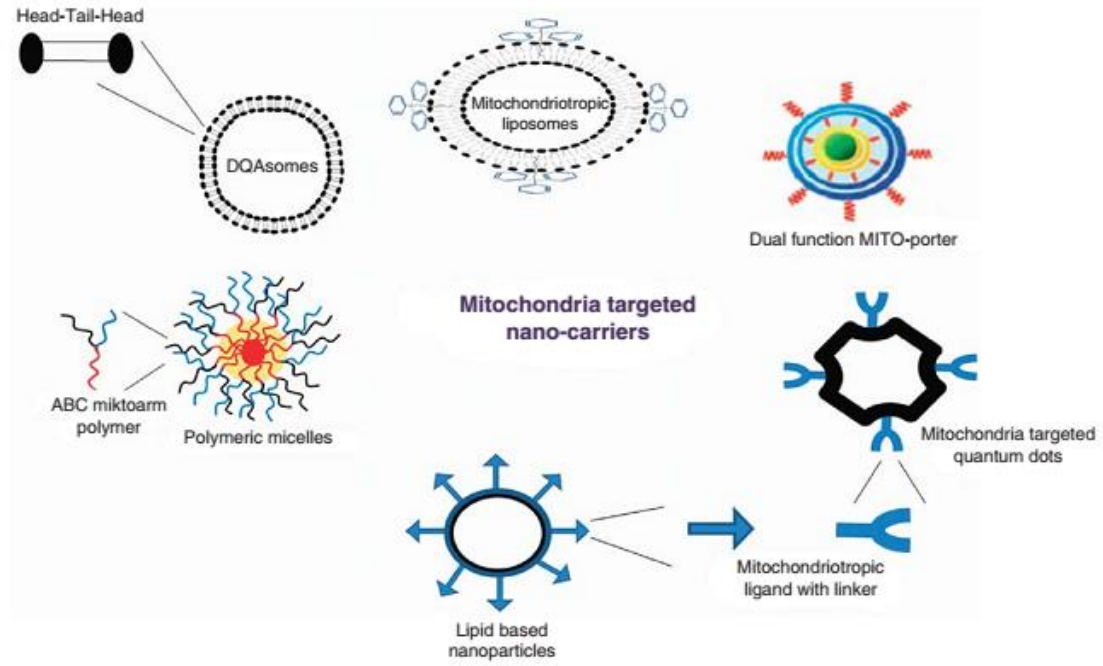

Figure 16 - **Nanocarriers with potential for mitochondrial targeting.** Adapted from (8).

The development of these new non-viral nanocarriers with affinity towards mitochondria has a great importance for mitochondrial disease treatment and approaches by MGT. Thus the main goal of this work was the construction of a novel non-viral nanocarrier with an mtDNA construct, obtained in our laboratory, with mitochondria affinity whose details are described in the next topic.

3.2.1. $CaCO_3$ Nanoparticles

Calcium carbonate ($CaCO_3$) is produced by many organisms forming unique structures with a variety of functions in their tissues. $CaCO_3$/DNA nanoparticles are produced by co-precipitation of Ca^{2+} with DNA in the presence of $CO3^{2-}$. This is an attractive method since it is a very a simple technique, promotes gene delivery with protection of the encapsulated DNA from degradation and the nanoparticles can be internalized into different histological cell types. However, $CaCO_3$/DNA precipitates are uncontrollable, resulting in large size nanoparticles which causes negative effects on cellular internalization and gene transfection (11,12,80).

$CaCO_3$ based nanoparticles have many advantages such as biocompatibility, biodegradability, loading ability of different therapeutic agents, easy and cheap production and pH dependent dissolution (9-11). To improve the stability and the transfection efficiency of $CaCO_3$ nanoparticles, natural compounds such as alginate and cellulose were used in the formulation of the nanoparticles. By changing the formulation, disadvantages like the uncontrollable growth of the nanoparticles could be slowed thus enhancing the stability of the

nanoparticles (11). To create $CaCO_3$/DNA nanoparticles with affinity towards mitochondria Rhodamine 123, a fluorescent amphiphile with mitochondria affinity was used (12,13).

In this work $CaCO_3$/pCAG-GFP-mtND1 nanoparticles were developed. The pCAG-GFP-mtND1 construct was successfully developed and produced in our laboratory for the development of the nanoparticles. The purpose of creating nanoparticles with this construct is the possible development of a therapeutic approach for PD disease, with efficient delivery of the construct to mitochondria. Also, a new polymer and its influence in the nanoparticles features was studied. This new polymer was gelatin, a natural polymer derived from collagen, with great advantages, such as, biocompatibility and biodegradability being suitable to be used in MGT (87).

Aims of the Project

Mitochondrial genome is considered very susceptible to mutations due to the lack of protection and repair mechanisms. Mutations in this genome are a frequent cause of mitochondrial cytopathies and conventional treatments, using a combination of different drugs, are in most cases, inefficient. The development of gene therapy to treat mtDNA disorders offers a promising approach; it is a practical and potentially effective tool to treat the vast array of clinical phenotypes as it focuses in the actual cause of the disorder. For mitochondrial gene therapy to be feasible in a clinical setting, the formulation of a carrier with mitochondrial targeting ability is imperative. In line with this, the aim of this project is the design and development of a mitochondrial gene based plasmid DNA vehicle suitable for efficient and targeted mitochondrial delivery. To accomplish this goal, the project was divided in three parts. The first involves the construction of a vector using an OXPHOS complex I gene, mtND1 and the pCAG-GFP plasmid. The second aim of this project was focused in the study of different hosts transformed with the pCAG-GFP-mtND1 vector to produce the plasmid. The third and last part, consisted in the formulation of a suitable nanocarrier for efficient and sustained pDNA delivery into mitochondria.

The success of this work is based in the development of a mtND1 gene based plasmid DNA loaded nanomaterial for mitochondrial gene therapy focused in complex I deficiency cytophaties.

Materials and Methods

1. Materials

1.1. Reagents

LB broth was obtained from Liofilchem (Roseto degli Abruzzi, Italy) and LB-Agar was obtained from Pronadisa/Conda (Madrid, Sapin). Yeast Extract was obtained from Himedia (Mumbai, India) and Tryptone was obtained from Biokar (France). Glycerol and $CaCl_2$ were obtained from VWR International (Radnor, PA, USA). KH_2PO_4 was obtained from Chem-Lab (Zedelgem, Belgium) and Na_2CO_3 and K_2HPO_4 were obtained from Panreac (Barcelona, Spain). Agarose and Green Safe were obtained from NZYTech (Lisboa, Portugal). Rhodamine 123 and Gelatin was from Sigma-Aldrich (St. Louis, MO, USA). Cellulose powder was obtained from Aldrich Chemical Company (Milwaukee, WI, USA). The plasmid pCAG-GFP was obtained from Addgene (Cambridge, MA, USA).

1.2. Hosts

In this work, different hosts were considered. *E. coli* XL1B, *E. coli* DH5α, *E. coli* JM109, *P. Pastoris* X33 and *S.cerevisiae* NRRL Y-12632 . As the pCGA-GFP gives ampicillin resistance, *P.Pastoris* X33 and *S.cerevisiae* were excluded from the study because of its resistance to ampicillin.

2. Methods

2.1. Vector construction

2.1.1. ND1 gene amplification

In its simplest form, polymerase chain reaction (PCR) based cloning is used to amplify a specific DNA sequence but at the same time it can be used to add restriction sites to the ends of that sequence, so that it can be easily cloned into a plasmid of interest.

Human mitochondrial DNA was extracted from blood samples and the mtND1 gene was amplified by PCR using the extracted mtDNA as template and the following primers: FW: GCAGAGCCCGGTAATCGCATA and RV: GGATTCTCAGGGATGGGTTC. The reagents used for the reaction were 1 U DreamTaq™ Green DNA polymerase (Fermentas, MA, USA), 2 mM $MgCl_2$, 0.2 mM dNTPs, 0.25 mM of each primer and 100-300 ng of mtDNA.

Table 3 - **Thermal cycling program for mtND1 PCR amplification.**

Step	Temperature	Time
1	95ºC	5 min
2	95ºC	30sec
3	60ºC	30sec
4	72ºC	40sec
	Repeat 35 times steps 2,3 e 4	
5	72ºC	8 min
6	12ºC	6min

The primers selected for mtND1 gene PCR created the desired enzyme cutting sites for enzyme digestion with SmaI and XbaI thus preventing the enzymes to cut any part of the gene.

2.1.2. Binding Reaction

For cloning mtND1 gene in pCAG-GFP (both previously digested with SmaI and XbaI) several ratios insert/vector were prepared. The key in these cloning reactions is to vary the insert concentration and maintain the vector concentration. To perform the binding reaction the following formula was used,

(ng vector x kb insert) / kb vector = ng insert ***(1)***

The ratios prepared were 1:1, 3:1, 5:1 and 8:1 using a DNA Ligation Kit (Takara Bio Inc., Otsu, Japan). The mixture consists in 36.7 ng of pDNA with 5 µL of Ligation Mix, ddH_20 and a variable amount of insert (depending on the ratio used) to a total volume of 10 µL. The ligation reaction mixture was incubated at room temperature for about 3h. Afterwards, the preparation of the desired construct was confirmed by sequencing,

2.2. Enzymatic digestion

The purified pCAG-GFP-mtND1 from several colonies was submitted to enzymatic digestion to verify if these colonies had the insert mtND1.

Different concentrations of pDNA (obtained from different selected colonies) were mixed with 2 µL of CutSmart® Buffer, 0.5 µL of SmaI (New Englands Biolabs, Ipswich, MA, USA), 0.5 µL of XbaI (New Englands Biolabs, Ipswich, MA, USA) and ddH_2O to a final volume of 10 µL.

The conditions for enzyme digestion used are displayed in table 4 and were conducted in a T100™ Thermal Cycler (Bio-Rad, CA, USA):

Table 4 - **Conditions for enzyme digestion.**

Enzyme	*Temperature*	*Time*	*Cut Type*	*Cutting sites*
SmaI	30ºC	1h	Blunt ends	5' CCC GGG 3' 3' GGG CCC 5'
XbaI	37 ºC	1h	"sticky" ends	5' T CTAGA 3' 3' AGATC T 5'

An agarose gel was done to verify if the digestion was correctly performed.

2.3. Sequencing

The pCAG-GFP-ND1 plasmid was obtained from fermentation of a selected colony and was sequenced by adapting the Beckman Coulter's GenomeLab™ Dye Terminator Cycle Sequencing protocol.

For preparation of the DNA sequencing reaction, about 50 fmol of purified pCAG-GFP were mixed with 0.3 µL of 0.25 µM primer (RV: EGFP-N CGTCGCCGTCCAGCTCGACCAG), 4 µL of DTCS Quick Start Master Mix and ddH2O to a final volume of 10 µL. The thermal cycling program used is displayed in table 5 and conducted in a T100™ Thermal Cycler (Bio-Rad, CA, USA):

Table 5 - **Thermal cycling program for DNA sequencing reaction.**

Step	**Temperature**	**Time**
1	98ºC	5 min
2	96ºC	20 sec
3	50ºC	20 sec
4	60ºC	4min
	Repeat 30 times steps 2,3 e 4	
5	60ºC	10 min
6	4ºC	6 min

After the thermal cycling, ethanol precipitation of the DNA sequencing reaction was promoted. To each reaction tube, 3 µL of Stop Solution/Glycogen mixture (1.2 µL of 3 M Sodium Acetate, pH 5.3, 1.2 µL of 100 mM Na2-EDTA, pH 8.0, and 0.6 µL of 20 mg/mL of glycogen) and 60 µL of chilled 95% (v/v) ethanol were added. This mixture was centrifugated at 3,000 rpm for 30 min. The obtained pellet was washed two times with chilled 70% (v/v) ethanol, with a centrifugation at 3,000 rpm for 5 min between each step. When dried, the pellet was

resuspended in 10 µL of Sample Loading Solution. The samples were transferred to the appropriate wells of the sample plate. Each of the samples were covered with a drop of light mineral oil. The samples for plasmid sequencing were loaded into the GenomeLab™ GeXP Genetic Analysis System (Beckman Coulter, California, USA). The primers used were RV: EGFP-N CGTCGCCGTCCAGCTCGACCAG for pCAG-GFP-mtND1 and FW: GCAGAGCCCGGTAATCGCATA and RV: GGATTCTCAGGGATGGGTTC for mtND1 gene. The primers used for the ligation product allowed to verify the existence of an insert in pCAG-GFP. MtND1 was sequenced to verify the successful cloning of the gene of interest in the plasmid.

2.4. Cell transformation

Transformation occurs when a cell captures foreign DNA from its surroundings. It can occur in nature in certain types of bacteria but when competent bacterial cells are used, they can be artificially transformed by a procedure called by heat shock method.

The ligation reaction mixture was used for transformation of *E.coli* DH5α competent cells by adding 10 µL of the ligation mixture to 100 µL of cells. After a short incubation in ice, the mixture was placed at 42°C for 45 seconds and then placed back in ice. LB medium was added and the transformed cells were incubated at 37 ºC for 2h in an orbital shaker at a shaking frequency of 250 rpm. Afterwards, the transformed cells were plated in LB agar plates (15g/L Agar, 10g/L Tryptone,5 g/L Yeast Extract, 5 g/L NaCl) complemented with 100 µg/mL ampicillin and 50 µg/mL neomycin and grew overnight at 37 ºC. After choosing the best insert/vector ratio (as indicated in section 2.1.2) *E.coli* JM109 and XL1B strains were also transformed with the vector pCAG-GFP-mtND1.

2.5. Cell Banks

Transformed strains were selected and grew overnight at 37 ºC in 25 mL LB medium (10g/L Tryptone,10 g/L NaCl, 5 g/L Yeast Extract; Sigma-Aldrich) complemented with 100 µg/mL ampicillin and 50 µg/mL neomycin in an orbital shaker at a shaking frequency of 250 rpm. When 0.7 of optical density (OD) at 600 nm was achieved, bank cells were made by adding 30% of glycerol, previously autoclaved, and stored at -80^{0}C for 3 to 4 days to stabilize.

2.6. Plasmid DNA production studies

These studies were carried out to verify which of the strains produced the pCAG-GFP-mtND1 with a better yield. The pCAG-mtND1 plasmid was produced in *E. coli* JM109, XL1B and DH5α strains in 125 mL of Terrific Broth (TB) medium (20 g/L tryptone, 24 g/L yeast extract, 4 mL/L glycerol, 0.017 M KH_2PO_4, 0.072 M K_2HPO_4) in 500 mL erlenmeyer complemented with 100 µg/mL ampicillin and 50 µg/mL neomycin at 37 ºC in an orbital shaker at a shaking frequency

of 250 rpm. The fermentations were carried out for 9.5 hours and samples of the culture media with an OD of 0.4 were taken every one and half hour. The samples were centrifuged at 13,000 rpm for 10 minutes in a Mikro 20 centrifuge (Hettich Centrifuges, UK), the supernatant was removed and cells were stored at -20 ºC for following purification. Three independent studies were made for each one of strains for triplicates.

2.7. Growth of pCAG-mtND1 for nanoparticle synthesis

The pCAG-mtND1 plasmid was produced in *E. coli* JM109 in 250 mL of Terrific Broth (TB) Medium (20 g/L tryptone, 24 g/L yeast extract, 4 mL/L glycerol, 0.017 M KH2PO4, 0.072 M K2HPO4) in 1000 mL erlenmeyer complemented with 100 µg/mL ampicillin and 50 µg/mL neomycin at 37 ºC in an orbital shaker at a shaking frequency of 250 rpm. After approximately 7 hours of fermentation, the cells were harvested by centrifugation for 10 min at 4 ºC and 4500 rpm in an Allegra 25R centrifuge (Beckman Coulter, CA, USA).

2.8. Plasmid Purification

2.8.1. Purification of the samples for yield studies

The purification was carried out using the GeneJet Plasmid Miniprep Kit (Thermo Scientific, Waltham, MA USA). This kit is designed for rapid and cost-effective small-scale preparation of high quality plasmid DNA from recombinant *E.coli* cultures.

Samples obtained from the culture media (described in section 2.6) were ressuspended and the cells were subjected to a SDS/alkaline lysis. The lysate was neutralised to create the conditions for posterior binding of pDNA on the silica membrane of the spin column. A centrifugation was made to obtain the cell debris and SDS in the pellet and the pDNA on the supernatant. The supernatant was loaded in the spin column membrane and, after elution, the membrane was washed a few times to remove contaminants. Finally the adsorbed pDNA was eluted with the elution buffer. The plasmid yield was determined by Uv-Vis analysis at 260 nm in a NanophotometerTM (Implen, Munich, Germany) and its integrity was confirmed by agarose gel electrophoresis. The purified pDNA was stored at -20ºC.

2.8.2. Purification of pCAG-GFP-mtND1 for nanoparticles production

NZYtech maxiprep (Nzytech, Lisboa, Portugal) kit is designed for the rapid, large-scale preparation of highly pure plasmid DNA from recombinant *E.coli* strains.

Previously harvested cells (described in 2.7 section) were ressuspended and a SDS/alkaline lysis was promoted. A neutralization solution was added and the sample was centrifuged for 30 min at 20.000 x g at 4ºC. The supernatant was transfered to a new tube and a 15 min centrifugation was made. The lysate was applied to the NZYTech Maxi Colunm and the elution occurred by gravity flow. The column was washed to remove contaminants and finally the pDNA was eluted. Precipitation of the eluted pDNA was promoted by adding 0.7 volumes of room-temperature isopropanol. A 20 min centrifugation at 15.000 x g was made and after, the pDNA was ressuspended in a pH 7.5 TE buffer. The plasmid yield was determined by spectrophotometry at 260 nm and its integrity was confirmed by agarose gel electrophoresis. 500 µL aliquots of pDNA at 100 µg/mL were prepared and stored at -80ºC.

2.9. Agarose gel electrophoresis

Agarose gel electrophoresis was performed to evaluate the size and conformation of the purified pCAG-GFP plasmid, to evaluate the size of mtND1 gene, the ligation product and to verify the enzymatic digestion of the ligation product.

The electrophoresis was carried out using a gel with 1% agarose and 1 µg/mL Green Safe and it was run at 150 V for 30 min in TAE buffer (40 mM Tris base, 20 mM acetic acid and 1 mM EDTA pH 8.0). The gel visualization was made in a UVItec Gel documentation system under UV light (UVItec Limited, Cambridge, United Kingdom).

2.10. Nanoparticles studies

2.10.1. $CaCO_3$ Nanoparticles Synthesis

For the nanoparticles synthesis, two different solutions were prepared: a solution A with 5 µg or 10 µg of pDNA, 120 µL of $CaCl_2$ (0.03 mg/mL) and 7.5 or 15 µL of $Rhodamine_{123}$ diluted with mili-Q water to a total volume of 290 µL and a solution B with 255 µL $NaCO_3$ (0.0425 mg/ml) and 5 µL of mili-Q water or cellulose (1mg/mL) or gelatin (1mg/mL) to a total volume of 260 µl.

Solution A was added dropwise with a micropipette to solution B to form the nanoparticles by a co-precipitation method. The final solution, called solution C, was centrifuged at 10,000 rpm for 15 min. The pellet contained the nanoparticles.

2.10.2. Particles Morphology

20 µL of tungsten 1% were added to the pellet obtained in the preparation of the nanoparticles by the method described in 2.10.1 and 1:20 and 1:50 dilutions were made. The

resulting solutions were set in roundly shaped 5 mm cover-slips and left at room temperature overnight to dry. In the following day, the samples were sputter coated with gold using an Emitech K550 sputter coater (London, England) and then analyzed by scanning electron microscope (SEM) (Hitachi S-2700, Tokyo, Japan), operated at an accelerating voltage of 20 kV with variable magnifications.

2.10.3. pDNA Encapsulation Efficiency

The encapsulation efficiency (EE) allows to determinate if the pDNA was efficiently loaded into the nanoparticle. EE was determined after centrifugation, following method described in 2.10.1, and recovery of the supernatant. The supernatant contains the pDNA that was not encapsulated into the $CaCO_3$ nanoparticles. The concentration of unbound pDNA was determined by Uv-vis analysis at 260 nm in a NanophotometerTM (Implen, Munich, Germany). Deionized water was used as blank for the measurements. The EE (%) was calculated by the equation,

$$\mathbf{EE\ (\%) = (pDNA_{total} - pDNA_{unbound})/pDNA_{total}} \quad \textit{(2)}$$

where $pDNA_{total}$ is the concentration of the pDNA used to form the nanoparticles and $pDNA_{unbound}$ is the concentration of the pDNA obtained in the supernatant. Three independent measurements were made.

2.10.4. Nanoparticles Size and Zeta (ζ) Potencial

The nanoparticles were produced following the method described in 2.10.1. and ressuspended in 750 µL of mili-Q water. The average size of the particles and the surface charges (zeta potential) were determined, at 25ºC, using a Zetasizer nano ZS and a zeta dip cell. Dynamic light scattering (DLS) using a He-Ne laser 633 nm with non-invasive backscatter optics (NIBS) and electrophoretic light scattering using a patented laser interferometric technique named M3-PALS (Phase analysis Light Scattering) were applied for particle size and zeta potential determination, respectively. The Malvern zetasizer software v 6.34 was used. The average values of size and zeta potential were calculated with the data obtained from three measurements and their standard deviations shown as ± SD.

2.10.5. Cell Citotoxicity

Before cell seeding, the plates were ultraviolet (UV) irradiated for 30 min. Plasmid DNA nanoparticles were applied to a 96-well plate (Nunc.). Human fibroblast were plated at confluency in 96 well plate, with 2×10^4 cells per well at 37 ºC in 5% CO_2 humidified atmosphere,

for 24, 48 and 72 h. After incubation, the redox activity was assessed through the reduction of the MTT. 100 µL of MTT dye solution (0.05 mg/mL in Krebs) was added to each well, followed by incubation for 2 hours at 37 ºC, in a 5% CO_2 atmosphere. The medium was aspirated and the cells were treated with 50 µL of isopropanol/HCl (0.04 N) for 30 minutes. Absorbance at 570 nm was measured using a Biorad Microplate Reader Benchmark. The spectrophotometer was calibrated to zero absorbance using the culture medium without cells. The relative cell viability (%) related to control wells was calculated by

$$[A]_{test}/[A]_{control} \times 100 \qquad (3)$$

where $[A]_{test}$ is the absorbance of the test sample and $[A]_{control}$ is the absorbance of control sample. Three independent measurements were made. The statistical analysis of experimental data used the Student's t-test and the results were presented as mean ± standard deviation (SD). Statistical significance was accepted at a level of $p < 0.05$.

Results

1. ND1 gene amplification

ND1 gene is a mitochondrial gene responsible for encoding an OXPHOS complex I protein. To obtain this gene, mtDNA was extracted from human blood and a PCR, with specific designed primers for sequence of mtND1 gene, was made. The purified PCR product was analyzed by agarose gel electrophoresis and sequenced, to verify its integrity, identity and purity. In this work, only was made a PCR amplification of the previously purified mtND1 gene to verify the primers efficiency.

The agarose gel electrophoresis (figure 17 lanes 3, 4 and 5) shows that the mtND1 gene is pure and that the PCR worked correctly. The mtND1 gene has 1200 bp which corresponds approximately to the 1000 bp DNA ladder lane.

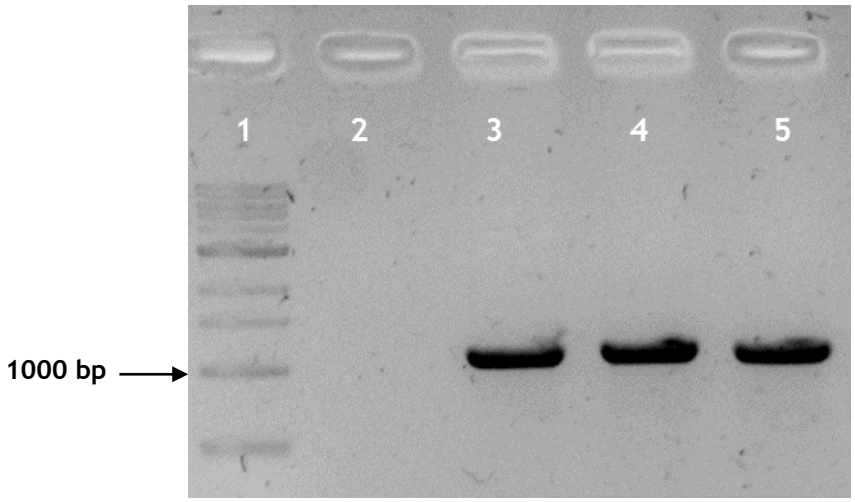

Figure 17 - **Agarose gel electrophoresis of mtND1 gene amplification by PCR.** Lane 1 –1 kb DNA Ladder (New England Biolab); Lane 2 – Negative control; Lane 3 – Positive control (mtND1 gene); Lane 4 and 5 – PCR product.

2. Plasmid Amplification and purification

2.1. pCAG-GFP-ND1 Agarose gel electrophoresis

When the desired pCAG-GFP-mtND1 construct was obtained, *E.coli* DH5α competent cells were transformed. After an overnight growth, a colony PCR of some selected colonies was made to verify if the mtND1 gene was present. To make colony PCR, the colonies were selected with a sterile micropipette tip and ressuspended in 5 µL of ddH_2O in a 1.5 mL centrifuge tube.

Lysis was promoted by placing the centrifuge tube at 100 ºC for 2 minutes. Thereafter, the PCR has been performed following the method previously described for ND1 gene amplification.

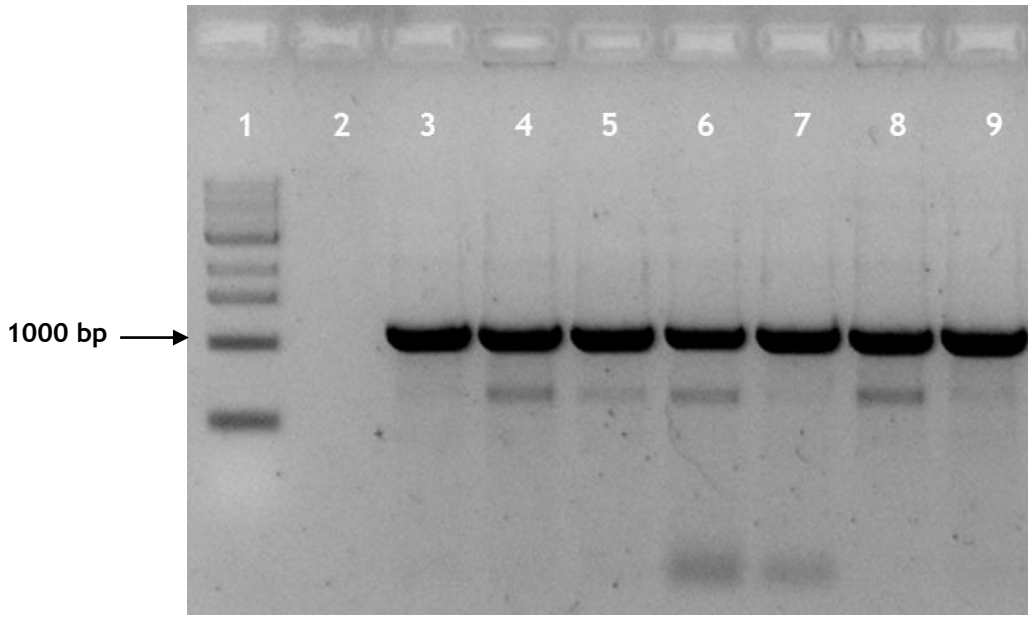

Figure 18 - **Colony PCR of E.coli DH5α colonies.** Lane 1 –1 kb DNA Ladder; Lane 2 – Negative control; Lane 3 to 9 - E.coli DH5α colonies with mtND1 gene amplification

An enzymatic digestion was made to the construct to verify if the mtND1 gene was actually present in some of the selected colonies (figure 19). In lanes 4 and 5 it was verified that the desired gene was present. This can be concluded by observing the lane that correspond to the mtND1 gene used as control and with the 1000 bp DNA ladder lane. The same colonies were used for pCAG-GFP-ND1 sequencing.

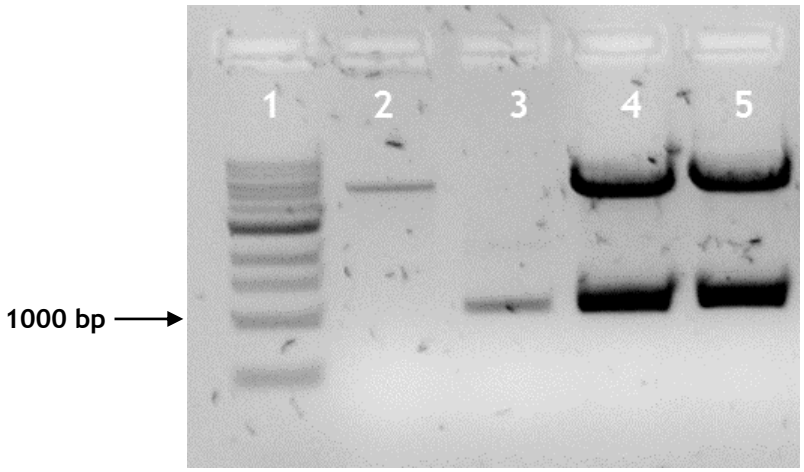

Figure 19 - **Enzymatic digestion of pCAG-GFP-mtND1 with SmaI and XbaI.** Lane 1 - 1 kb DNA Ladder; Lane 2 - pCAG-GFP; Lane 3 - mtND1 gene, Lane 4 and 5 - E.coli DH5α colonies with pCAG-GFP-ND1

2.2. pCAG-GFP-ND1 sequencing

DNA sequencing provides the complete characterization of a recombinant plasmid. Primers targeting the plasmid backbone and the insert sequence should be used and the identification and order of the given DNA can be determined. When working with recombinant constructs the sequencing allows us to confirm the DNA sequence of the insert and also to examine the junctions between the plasmid and insert. The most used technique for recombinant plasmids is Sanger sequencing. This technique involves the use of a DNA polymerase, primers, unlabeled deoxynucleotide triphosphates (dNTPs), and fluorescently labeled dideoxynucleotide triphosphates (ddNTPs). When a ddNTP is incorporated into a newly synthesized strand, the addition of more nucleotides is stopped, thus resulting in a DNA product with a fluorescently labeled ddNTP at the end of the strand. The sequence of nucleotides can then be determined by separating the DNA products by size.

A transformed *E.coli* DH5α colony was selected for sequencing and the purified pDNA was prepared for sequencing analysis with the method previously described. The sequencing results are shown in figure 20.

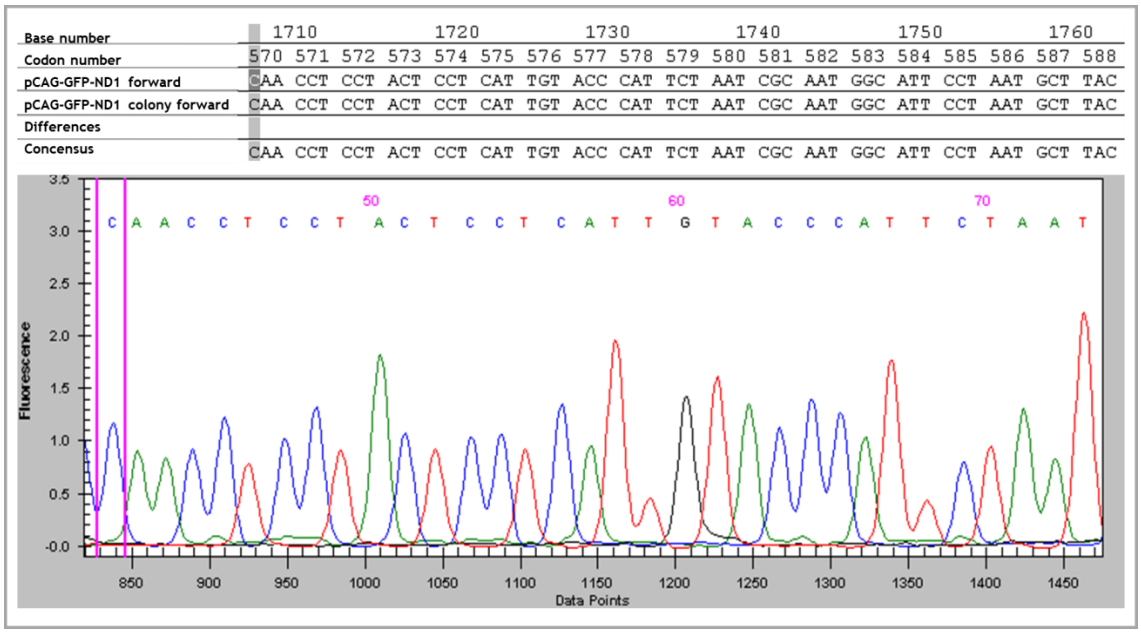

Figure 20 - **pCAG-GFP-mtND1 sequencing obtained from E.coli DH5α transformed colony.** The mtND1 sequence was obtained from GenBank, accession number NC_012920, region 3307 to 4262.

These results demonstrate that the mtND1 gene sequence is the same of the obtained from GenBank showing that the gene is present on the pCAG-GFP and that its integrity was maintained.

3. Host studies

Several studies using different recombinant hosts could be made when working with a plasmid construct, also depending on the purpose of the work. Normally if a plasmid large scale production is required, prokaryotic cells like *E. coli* are used. When the purpose is to obtain a large scale recombinant protein production, eukaryotic cells like *P. pastoris and S. cerevisiae* could be used. It is important to isolate the transformed cells from the ones that do not contain the construct. Generally, plasmids are created with one or more specific genes such as antibiotic resistance genes, which permit a selective isolation of the transformed cells. An important aspect when choosing a plasmid and a host is to analyze all these aspects.

In this work, the host studies had the purpose to evaluate if a plasmid with an mtDNA gene could be produced in different types of hosts. Different strains of *E.coli* (JM109, DH5α and XL1B), *P. Pastoris* X33 and *S. cerevisiae* NRRL Y-12632 were chosen as hosts for the pCAG-GFP-mtND1 production.

3.1. *P. pastoris* X33 and *S. cerevisiae* NRRL Y-12632

Before proceeding to the cell transformation, *P. Pastoris* X33 and *S. cerevisiae* NRRL Y-12632 were plated on YPD (10 g/L yeast extract, 20 g/L peptone, 20 g/L dextrose and 20 g/L Agar) plates complemented with 100 µg/mL ampicillin and left at 30 ºC overnight. Cell growth was observed and YPD plates complemented with 500 µg/mL ampicillin were made. In figure 21it can be seen that *P. pastoris* X33 and S. *cerevisiae* NRRL Y-12632 demonstrated resistance to ampicillin. Because pCAG-GFP-mtND1 gives the ampicillin resistance, thus that being the only way to isolate the colonies with the construct, *P. pastoris* X33 and S. *cerevisiae* NRRL Y-12632 were excluded from the studies.

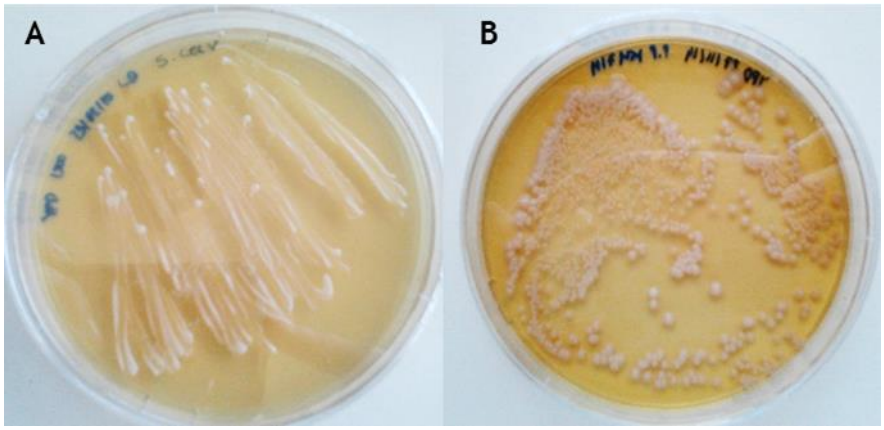

Figure 21 **- Growth of P. *pastoris* X33 and S. *cerevisiae* NRRL Y-12632 on YPD plates complemented with 500 µg/ml ampicillin.** A - S. *cerevisiae* NRRL Y-12632 B - P. *Pastoris* X33.

3.2. *E. coli* JM109, XL1B and DH5α

In order to perform the cell growth and plasmid production studies, bank cells with *E.coli* JM109, DH5α and XL1B transformed with the pCAG-GFP-mtND1 were prepared. Fermentations were carried out as previously described and optical density at 600 nm was measured every one and half hour. Cell samples were also recovered at each time point to further analyse the pDNA production level. By analyzing the growth curves, the samples of *E.coli* cells taken at 1.5, 4.5 and 7.5 hours were selected for pDNA purification and quantification. To calculate the pDNA specific yields, cell dry weight (CDW) for each one of the strains was determined by performing fermentations in the same conditions and by taking 1 mL sample every hour with the correspondent OD measurement. The samples were centrifuged at 13000 rpm for 10 minutes, the supernatant was removed and the cell pellets were placed at 65 ºC during two days until constant weight was reached. The centrifuge tubes were weighted empty and after cells recovery, allowing the calculation of the specific cell dry weight for all the strains. It was verified that 1 OD unit corresponded to 0.36 g CDW for JM109 strain, to 0.35 g CDW for DH5α and to 0.33 g CDW for XL1B.

The growth curves profiles of the *E. coli* strains were very similar, all reaching approximately an OD of 4 in 9.5 hours of fermentation. When analyzing the pDNA specific yield, one can see that there are some differences. JM109 demonstrated to have the better pDNA specific yields and XL1B pDNA specific yields decreased over time (Figures 22-24).

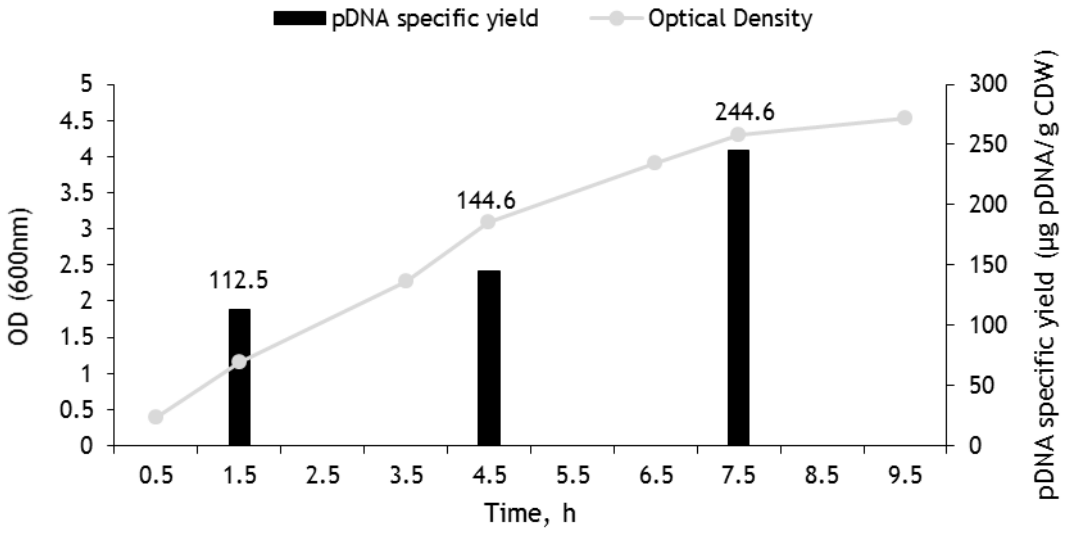

Figure 22 - **Growth curve of E.*coli* JM109 transformed with pCAG-GFP-mtND1.** Plotted is the optical density at 600 nm as a function of time in hours. pDNA specific yield was measured at 1.5, 4.5 and 7.5 hours. Data was obtained from three independent measurement

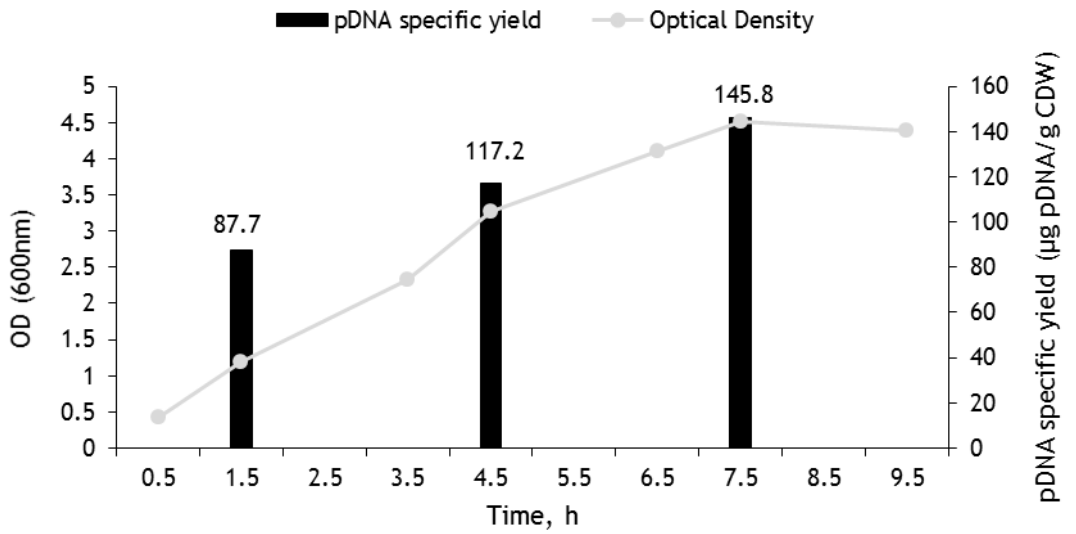

Figure 23 - **Growth curve of E.*coli* DH5α transformed with pCAG-GFP-mtND1.** Plotted is the optical density at 600 nm as a function of time in hours. pDNA specific yield was measured at 1.5, 4.5 and 7.5 hours. Data was obtained from three independent measurements.

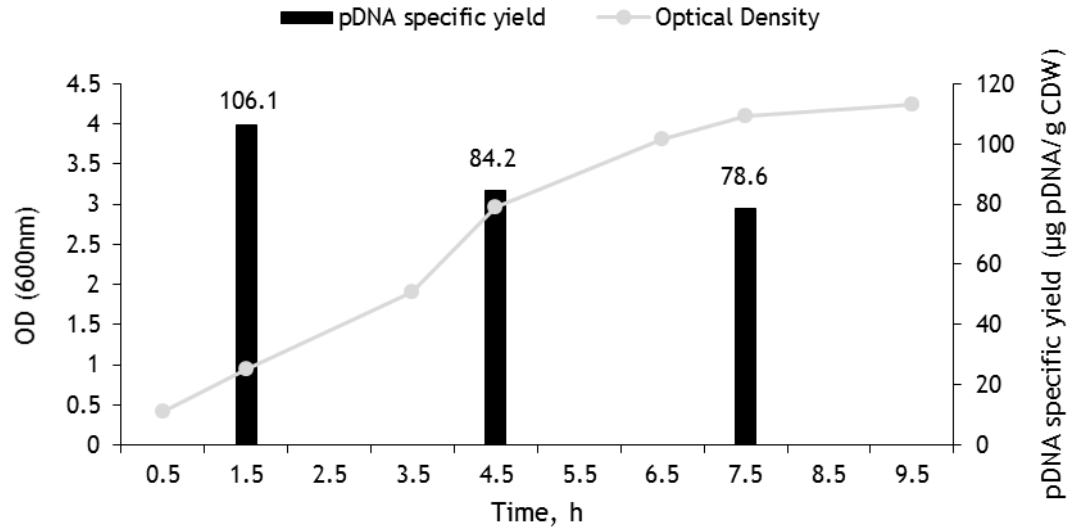

Figure 24 - **Growth curve of E.*coli* XL1B transformed with pCAG-GFP-mtND1.** Plotted is the optical density at 600 nm as a function of time in hours. pDNA specific yield was measured at 1.5, 4.5 and 7.5 hours. Data was obtained from three independent measurements.

4. $CaCO_3$ Nanoparticles synthesis

$CaCO_3$ nanoparticles are very easy to produce, are biocompatible and biodegradable. The $CaCO_3$/pDNA nanoparticles are obtained by a method called co-precipitation where a solution with $CaCl_2$ and pDNA is added to a solution with $CaCO_3$. When the Ca^{2+} plus pDNA is in the presence of $CO3^{2-}$ the desired nanoparticles are produced creating a precipitate that can be easily obtained by centrifugation. The $CaCO_3$ nanoparticle synthesis protocol was adapted from Santos and co-workers (12) and the process is schematized in figure25

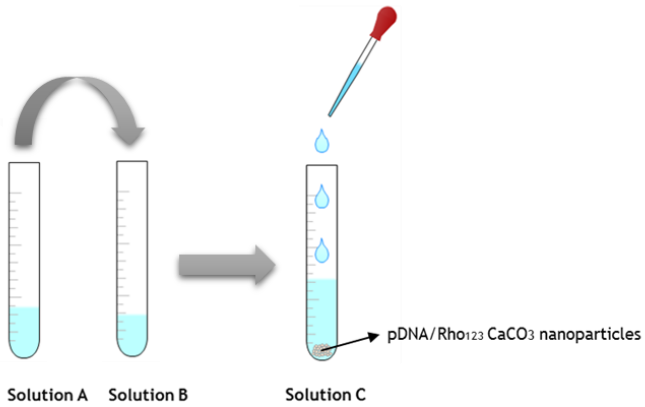

Figure 25 **- $CaCO_3$ Nanoparticles synthesis.** Solution A contains $CaCl_2$, pCAG-GFP-mtND1 and $Rhodamine_{123}$. Solution B contains Na_2CO_3, Cellulose or Gelatin. Solution C contains pDNA/Rho_{123} $CaCO_3$ nanoparticles that are formed by co-precipitation when solution A is added to solution B.

Two polymers were used for the production of pDNA/Rho_{123} $CaCO_3$ nanoparticles. In solution B cellulose or gelatin were added, in order to improve the properties of the nanoparticles concerning size reduction and stability. Rhodamine 123 was used because of its affinity towards mitochondria.

5. Encapsulation Efficiency

When aiming the therapeutic applications, it is important that a significant amount of the therapeutic plasmid reaches the target. The encapsulation efficiency (EE) permits to evaluate if the therapeutic plasmid was efficiently loaded in the nanoparticles. The EE was calculated for all the nanoparticles systems under study and is represented in table 6. All the systems presented higher than 50% of loading efficiency of pDNA which is a very important feature because a good amount of pDNA should reach mitochondria to have a beneficial effect on its function. Previously, both Santos and co-workers and Salvado and co-workers (12,13) obtained similar results with the same co-precipitation method. These results showed that the nanoparticles produced by these method have a good encapsulation efficiency (above 50%) when prepared with plasmids with different sizes.

Table 6 - **Loading efficiency of pCAG-GFP-mtND1/Rho_{123}, pCAG-GFP-mtND1/Rho_{123}/cellulose and pCAG-GFP-mtND1/Rho_{123}/gelatin $CaCO_3$ nanoparticles with 5 µg and 10 µg pCAG-GFP-mtND1 loading amount.** The values of encapsulation efficiency were calculated with the data obtained from three independent measurements (mean ± SD, n = 3).

$CaCo_3$ Nanoparticles	*Loading efficiency of pDNA*
5 µg pCAG-GFP-mtND1/Rho_{123}	58.39 ± 1.76
10 µg pCAG-GFP-mtND1/Rho_{123}	60.41 ± 1.58
5 µg pCAG-GFP-mtND1/Rho_{123}/cellulose	51.21 ± 1.52
10 µg pCAG-GFP-mtND1/Rho_{123}/cellulose	58.36 ± 1.36
5 µg pCAG-GFP-mtND1/Rho_{123}/gelatin	54.58 ± 0.51
10 µg pCAG-GFP-mtND1/Rho_{123}/gelatin	53.01 ± 1.05

Chen and co-workers (88) studied the DNA encapsulation efficiencies of $CaCO_3$/DNA co-precipitates prepared with different Ca^{2+}/CO_3^{2-}. They observed that the encapsulation efficiency increases with decreasing Ca^{2+}/CO_3^{2-} ratio in the high Ca^{2+}/CO_3^{2-} ratio range, showing that DNA could be fully encapsulated in the CaCO3/DNA co-precipitates if the amount of $CO3^{2-}$ used for preparing the co-precipitates is high enough. This could be a good approach for further studies for improvement of the encapsulation efficiencies.

6. Nanoparticle Size and Zeta potential (ζ)

Size and morphology of pCAG-GFP-mtND1/Rho_{123}/$CaCO_3$ nanoparticles were evaluated using Scanning Electron Microscopy. Two different concentrations of pCAG-mtND1 (5 µg and 10 µg) and two different polymers (cellulose and gelatin) were studied. The samples were shown to have some polydispersity in size but the same spherical shape morphology was observed (figures 26-28).

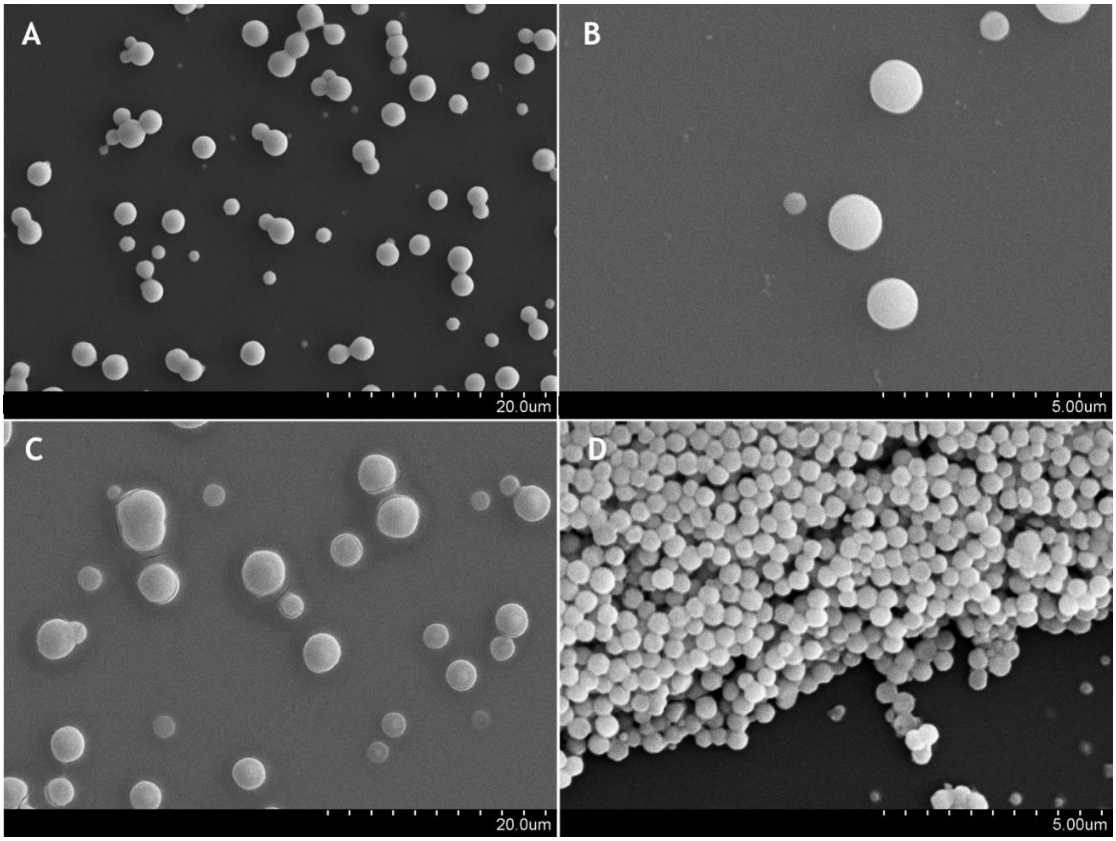

Figure 26- **pCAG-GFP-mtND1/Rho$_{123}$ CaCO$_3$ nanoparticles.** A and B - 5ug pDNA; C and D -10ug pDNA.

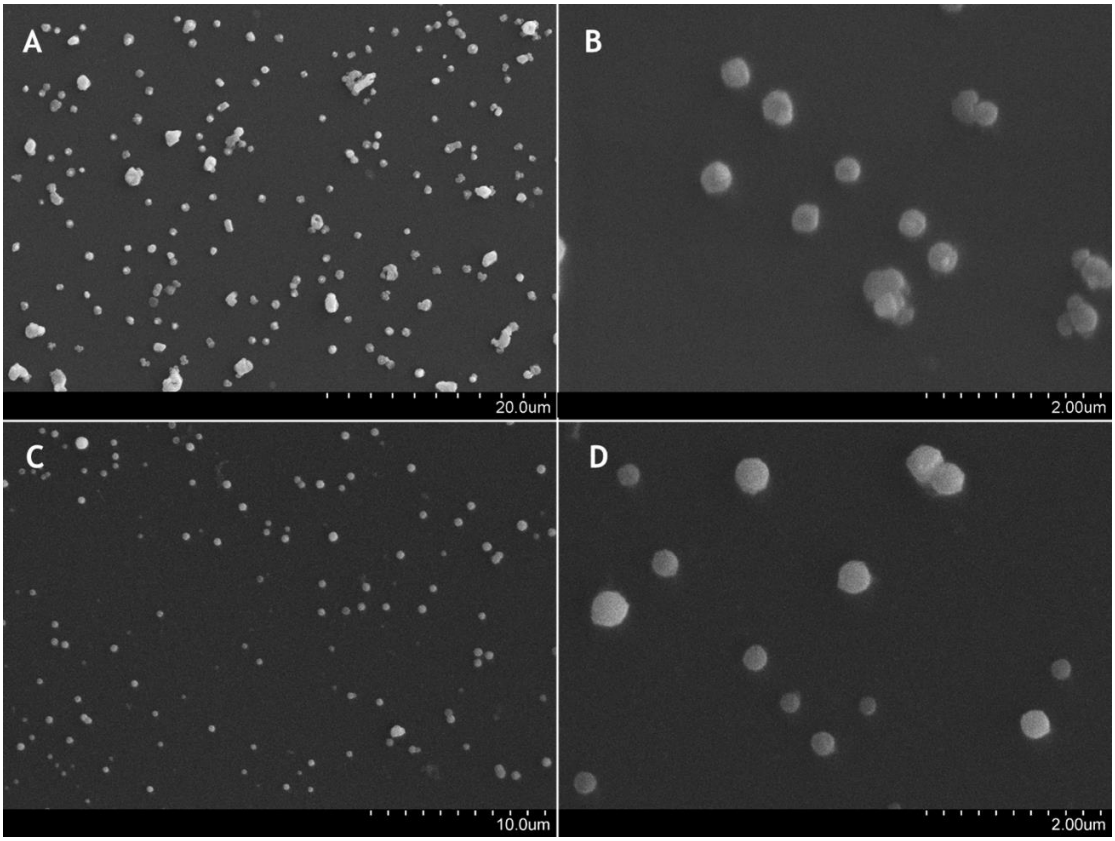

Figure 27 - **pCAG-GFP-mtND1/Rho$_{123}$/gelatin CaCO$_3$ nanoparticles.** A and B - 5ug pDNA; C and D -10ug pDNA.

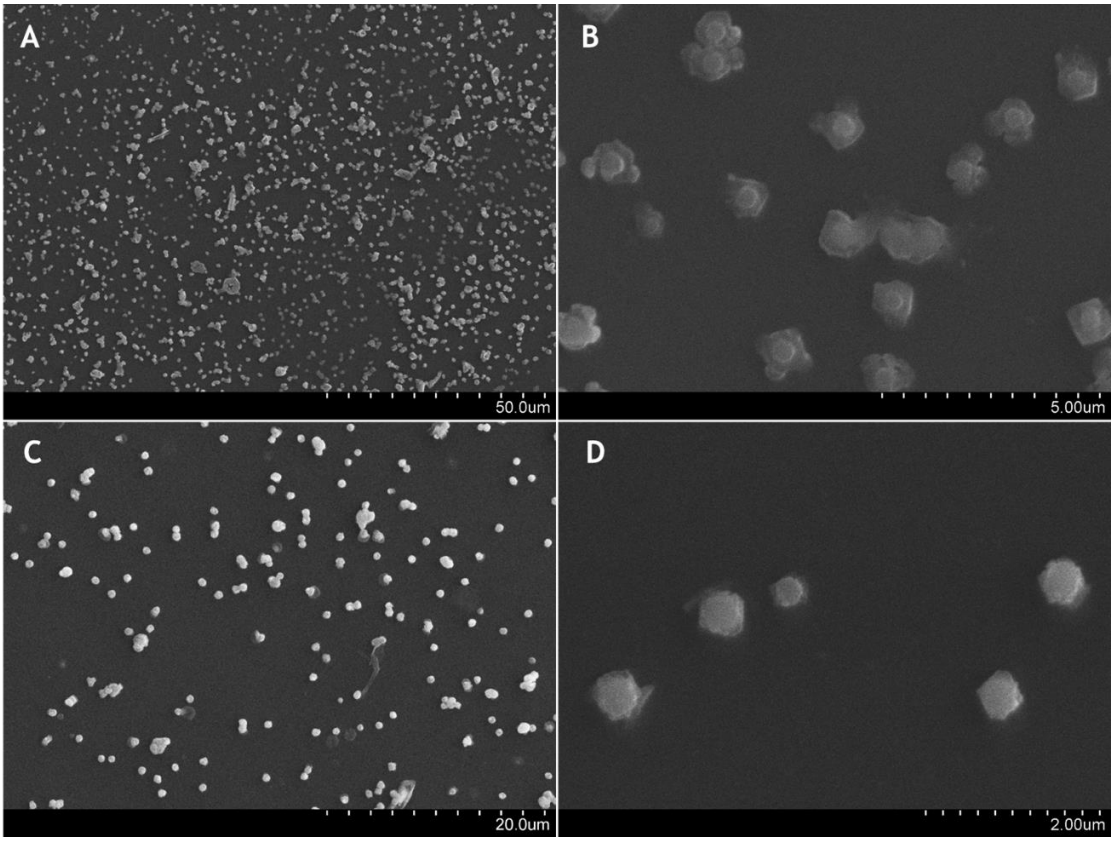

Figure 28 - **pCAG-GFP-mtND1/Rho123/cellulose CaCO3 nanoparticles.** A and B - 5ug pDNA; C and D - 10ug pDNA

The average size and zeta potential of the nanoparticles was measured using Zetasizer nano ZS (table 7). The nanoparticles presented sizes ranging between 141 nm to 282 nm. Practically all the particles had positive zeta potentials, with exception of the 10 µg pCAG-GFP-mtND1/Rho_{123}/cellulose system. Nanoparticle uptake by cells is dictated by its size (100-200 nm) and positive charge (to interact with the negatively charged cellular membrane) making the obtained nanoparticles suitable for cellular internalization and posterior interaction with mitochondria.

Table 7 - **Average size and zeta potential of pCAG-GFP-mtND1/Rho1$_{23}$, pCAG-GFP-mtND1/Rho$_{123}$/cellulose and pCAG-GFP-mtND1/Rho$_{123}$/gelatin $CaCO_3$ nanoparticles with 5 µg and 10 µg pDNA loading amount.** Average zeta potential values of pCAG-mtND1, free rhodamine 123, cellulose and gelatin are also presented. The values of zeta potential and size were calculated with the data obtained from three independent measurements (mean ± SD, n = 3).

System	*Particle size (nm)*	*Zeta Potential (mV)*
5 µg pCAG-GFP-mtND1/Rho$_{123}$/cellulose	282 ± 9.2	+29.7 ± 0.5
10 µg pCAG-GFP-mtND1/Rho$_{123}$/cellulose	212 ± 8.9	-10.1 ± 2.2
5 µg pCAG-GFP-mtND1/Rho$_{123}$/gelatin	196 ± 14.9	+51.4 ± 9.6
10 µg pCAG-GFP-mtND1/Rho$_{123}$/gelatin	141 ± 10.6	+39.8 ± 4.1
	Zeta Potential (mV)	
Rhodamine 123	+62 ± 1.1	
Cellulose	-89 ± 1.4	
Gelatin	+71 ± 8.9	

7. Cell Citotocixity

MTT is a yellow, water-soluble, tetrazolium salt. The MTT assay is a simple non-radioactive colorimetric assay to measure cell cytotoxicity or viability. Metabolically active cells are able to convert this dye into a water-insoluble dark blue formazan by reductive cleavage of the tetrazolium ring. The formed crystals can be dissolved and quantified by measuring the absorbance of the solution at 570 nm.

Cell viability is influenced by various chemical and physical proprieties of the nanoparticles including surface charge, composition, shape and size of the nanoparticles. Costa and co-workers (89) studied the cell cytotoxicity of pDNA microgels in human fibroblasts. They obtained cell viability values between 84-92% in human fibroblasts after 48 hours, concluding that these results were very satisfactory and that the microgels didn't have an acute cytotoxic effect thus not promoting an inflammatory response and having no influence in normal cell growth and function.

In our systems we obtained similar cell viability results with human fibroblasts. Although in the first 24 hours the 5 µg pDNA and 10 µg pDNA systems displayed a cell viability decrease of 13% and 16% respectively, after 72 hours both systems had an 83% cell viability. These results show that both systems induce low cell cytotoxicity, thus being biocompatible, a very important feature when aiming for gene therapy purposes.

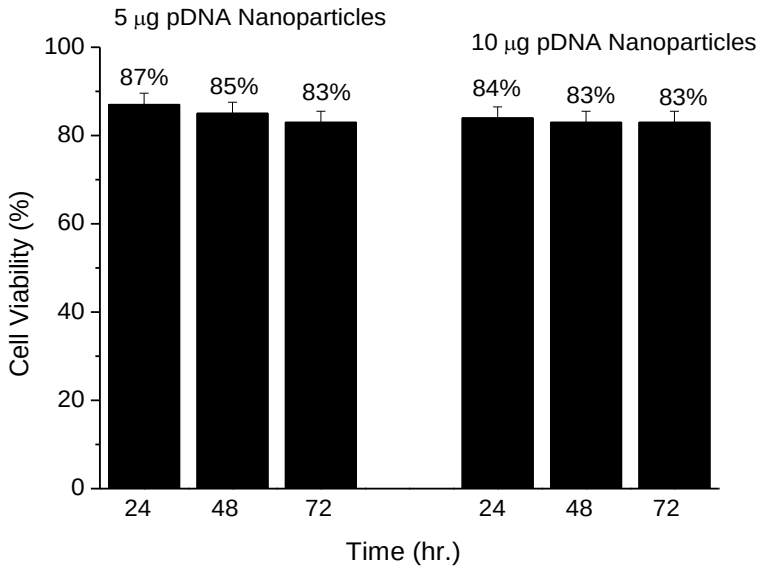

Figure 29 - **Cytotoxicity profile of 5 μg pDNA and 10 μg pDNA of pCAG-GFP-mtND1/Rho$_{123}$ $CaCO_3$ nanoparticles on human fibroblast cells after 24, 48 and 72 hours incubation, measured by the MTT assay.** The percentage viability is expressed relative to control cells (100% cell viability). The data were obtained by averaging the results from 3 experiments. The respective errors were determined as below 0.05%. The error bars in the figure represent the standard deviations (i.e. ± SD) from the 3 experiments.

Discussion

Mitochondrial genome is particularly vulnerable to mutations because of its proximity to ROS generation sites (66) and more than 250 pathogenic mtDNA mutations have been described (67). Currently no specific pharmaceutical drugs shown to treat mitochondrial disease effectively in large-scale clinical trials (69) thus gene therapy arises as a new approach to treat mitochondrial diseases. As no recombinant human mtDNA constructs are available (4) the design of a mtDNA construct, able for cellular transfection and consequent protein expression, is an exciting area of research and it will bring innovative features in mitochondrial therapeutics.

In this project, the aim was the development of a mitochondrial gene based plasmid loaded vehicle to be used in mitochondrial gene therapy protocols. The project starts with the development of a mitochondrial gene (mtND1) based plasmid and its production using different *E. coli* strains and proceeded with the encapsulation of this therapeutic plasmid into a nanoformulation. This system was then characterized concerning parameters such as size, morphology, surface charge, encapsulation efficiency and cytotoxicity.

Firstly, the vector was constructed by performing a binding reaction of the selected plasmid, pCAG-GFP with the mtND1 gene. Plasmid and gene were both subjected to the same enzymatic reaction using the restriction enzymes, SmaI and XbaI. Because the primers selected for mtND1 PCR were designed to add specific enzyme restriction sites, the gene sequence was not affected. After promoting a binding reaction with several plasmid/gene ratios, the construct obtained was inserted in *E.coli* competent cells. For all the ratios considered, growth was observed and because pCAG-GFP confers ampicillin resistance it could be assumed that the colonies that grown in the LB plates supplemented with 100 mg/mL ampicillin acquired the pCAG-GFP-mtND1 construct. The following step was to verify if the nucleotide sequence of the construct was maintained through cell division. After enzymatic digestion by doing an agarose gel it was observed that lanes corresponding to mtND1 gene and pCAG-GFP were present in some of the colonies selected. Sequencing showed that the construct was successfully obtained.

Secondly the vector needed to be amplified for posterior studies. Because it was observed a smaller *E.coli* growth with this construct, up to an OD of 4-5, growth and yield studies were carried out with different *E.coli* strains. The strains used were JM109, XL1B and DH5α. Although all of them presented similar growth curves, *E.coli* JM109 strain demonstrated to be more efficient in pCAG-GFP-mtND1 production. According to these results, *E.coli* JM109 was chosen for vector amplification.

The third and final step in this work consisted in the nanoparticles production and characterization. $CaCO_3$/pDNA nanoparticles were produced by co-precipitation of Ca^{2+} with DNA in the presence of $CO3^{2-}$. The influence of different polymers, cellulose and gelatin, on nanoparticles formation and characterization was studied. Cellulose and gelatin are commonly used in many pharmaceuticals formulations because of its biodegradability and biocompatibility. The purpose of using these polymers was to improve the nanoparticle's characteristics such as size reduction and stability. Rhodamine 123 was also used, because of

its affinity towards mitochondria. In nanoparticles characterization size, zeta potential, encapsulation efficiency and cell cytotoxicity were studied.

When it comes to size, scanning electron microscopy allowed to verify that all the nanoparticles had some polydispersity in size but the same spherical shape morphology. The average size presented by the nanoparticles with the polymers was between 282 nm and 141 nm and most of them had positive zeta potential values. These features are ideal for cell uptake and internalization taking into account the cell membrane properties (negative charge and nanoscale pores). Besides, because of the negative membrane potential of mitochondria, with a positive zeta potential the nanoparticles have a greater chance of reaching efficiently mitochondria. When analyzing the pDNA loading of the nanoparticles, one can see that EE from 51% to 68% were obtained, being EE slightly higher in nanoparticles without adding the polymers. No relevant differences were observed between the two polymers although the 10 ug pCAG-GFP-mtND1/Rho_{123}/cellulose system was the one that had a higher EE (58%). In general, all EE are above 50% which makes them suitable for gene therapy purposes. It is crucial, that a good amount of the mtDNA construct reaches mitochondria, for the desired beneficial effect on mitochondrial function be obtained.

Cell cytotoxicity of $CaCO_3$ nanoparticles with cellulose were previously studied by Santos and co-workers (12) (cell viabilities above 70%) and gelatin is a biocompatible and biodegradable natural polymer. Thus, cell cytotoxicity was evaluated by using nanoparticles without polymers. The nanoparticles had very low cell cytotoxicity with 83% of cell viability after 72h, showing that they can be used as suitable systems for gene therapy procedures.

In sum, these results demonstrated that a MGT construct can be produced and encapsulated in $CaCO_3$ nanoparticles with very promising features.

Conclusions and Future Perspectives

In this work an mtDNA gene, mtND1, was successfully cloned into pCAG-GFP, used to further transform *E. coli cells*. To the best of our knowledge, this is the first time a mitochondrial gene is successfully cloned into a plasmid opening a new range of possibilities to improve the therapeutics of mitochondrial diseases.

When producing the pCAG-GFP-mtND1 construct was observed that *E.coli* strains did not reached very high growth, achieving only ODs of 4-5. One can conclude that the construct in some way influences the growth of this strains.

pCAG-GFP-mtND1 plasmid based nanoparticles were formulated following a co-precipitation method. All nano-systems presented spherical and/or globular morphology, adequate sizes and positive zeta potential values while they are biocompatible and therefore very suitable for MGT.

Further studies should focus on *in vitro* studies concerning cell internalization and uptake and mainly on the delivery of the construct to mitochondria and the consequent expression of mtND1 gene.

One can conclude that this work was a great achievement for advances in mitochondrial gene therapy field. As being MGT an emerging field and an important approach for mitochondrial disease treatment, it is imperative to study new and improved methods to obtain mtDNA constructs and appropriate delivery systems that can easily and specifically reach mitochondria to efficiently deliver the construct.

Bibliography

1. Bigger, B. W., Liao, A. Y., Sergijenko, A., Coutelle, C. Trial and error: How the unclonable human mitochondrial genome was cloned in yeast. *Pharmaceutical Research*. 2011; *28*(11): 2863–2870.

2. Mukhopadhyay, A., Weiner, H. Delivery of drugs and macromolecules to mitochondria. *Advanced Drug Delivery Reviews*. 2007; *59*(8): 729–38.

3. Nunnari, J., Suomalainen, A. Mitochondria: in sickness and in health. *Cell*. 2012; *148*(6): 1145–59.

4. Doyle, S. R., Chan, C. K. Mitochondrial gene therapy: an evaluation of strategies for the treatment of mitochondrial DNA disorders. *Human Gene Therapy*. 2008; *19*(12): 1335–1348.

5. Dowling, D. K. Evolutionary perspectives on the links between mitochondrial genotype and disease phenotype. *Biochimica et Biophysica Acta*. 2014; *1840*(4), 1393–403.

6. Taylor, R. W. Gene therapy for the treatment of mitochondrial DNA disorders. *Expert Opinion on Biological Therapy*. 2005; *5*(2): 183–194.

7. Adhya, S., Mahato, B., Jash, S., Koley, S., Dhar, G., Chowdhury, T. Mitochondrial gene therapy: The tortuous path from bench to bedside. *Mitochondrion*, 2011; *11*(6): 839–44.

8. Malhi, S. S., Murthy, R. S. R. Delivery to mitochondria: a narrower approach for broader therapeutics. *Expert Opinion on Drug Delivery*. 2012; *9*(8): 909–935.

9. Ma, X., Li, L., Yang, L., Su, C., Wang, K., Jiang, K. Preparation of hybrid $CaCO_3$–pepsin hemisphere with ordered hierarchical structure and the application for moval of heavy metal ions. *Journal of Crystal Growth*. 2012; *338*(1): 272–279.

10. Liang, P., Zhao, D., Wang, C. Q., Zong, J. Y., Zhuo, R. X., Cheng, S. X. Facile preparation of heparin/CaCO3/CaP hybrid nano-carriers with controllable size for anticancer drug delivery. *Colloids and Surfaces B: Biointerfaces*. 2013; *102*: 783–788.

11. Zhao, D., Liu, C., Zhuo, R., Cheng, S. Alginate/$CaCO_3$ Hybrid Nanoparticles for Efficient Codelivery of Antitumor Gene and Drug. *Molecular Pharmaceutics*. 2012.

12. Santos, J., Sousa, F., Queiroz, J., Costa, D.. Rhodamine based plasmid DNA nanoparticles for mitochondrial gene therapy. *Colloids and Surfaces B: Biointerfaces*. 2014; *121*: 129–140.

13. Salvado, R., Sousa, F., Queiroz, J., & Costa, D.. Development of mitochondrial targeting plasmid DNA nanoparticles: Characterization and in vitro studies. *Colloids and Surfaces A: Physicochemical and Engineering Aspects*. 2014; *480*, 287–295.

14. Yu-Wai-Man, P., Griffiths, P. G., Chinnery, P. F. Mitochondrial optic neuropathies - Disease mechanisms and therapeutic strategies. *Progress in Retinal and Eye Research*. 2011; *30*(2): 81–114.

15. Cooper, G. M. The Cell: A Molecular Approach. 2nd edition, 2000, Sunderland (MA).

16. Wongrakpanich, A., Joiner, M. A., Anderson, M. E., & Salem, A. K. Mitochondria-targeting particles. 2014; *9*: 2531–2543.

17. Federico, A., Cardaioli, E., Da Pozzo, P., Formichi, P., Gallus, G. N., Radi, E.. Mitochondria, oxidative stress and neurodegeneration. *Journal of the Neurological Sciences*. 2012; *322*(1-2): 254–262.

18. Moreira, P. I., Zhu, X., Wang, X., Lee, H., Nunomura, A., Petersen, R. B., Perry, G., Smith, M. A. Mitochondria: A Therapeutic Target in Neurodegeneration. Biochim Biophys Acta. 2010; *1802*(1): 212–220.

19. Smeets, H. J. M.. Preventing the transmission of mitochondrial DNA disorders: Selecting the good guys or kicking out the bad guys. *Reproductive BioMedicine Online*. 2013; *27*(6): 599–610.

20. Lodish, H., Berk, A., Zipursky, S. L., Matsudaira, P., Baltimore, D. and Darnell J. Molecular Cell Biology. 4th edition, 2000, New York.

21. Chinnery, P. F., & Hudson, G. Mitochondrial genetics. *British Medical Bulletin*. 2013; *106*(1): 135–159.

22. Nicholls, T. J., & Minczuk, M.. In D-loop: 40years of mitochondrial 7S DNA. *Experimental Gerontology*. 2014; *56*: 175–181.

23. Stumpf, J. D., & Copeland, W. C. Mitochondrial DNA replication and disease: insights from DNA polymerase γ mutations. *Cellular and Molecular Life Sciences*. 2011; *68*(2): 219–233.

24. Shokolenko, I. N., Alexeyev, M. F. Mitochondrial DNA: A disposable genome? *Biochimica et Biophysica Acta (BBA) - Molecular Basis of Disease*. 2015; *1852*(9): 1805–1809.

25. Holt, I. J., Reyes A. Human Mitochondrial DNA Replication. Cold Spring Harb Perspect Biol. 2012; 4: a012971

26. McKinney, E. a., & Oliveira, M. T. Replicating animal mitochondrial DNA. *Genetics and Molecular Biology*. 2013; *36*(3): 308–315.

27. Alexeyev, M., Shokolenko, I., Wilson, G., LeDoux, S. The maintenance of mitochondrial DNA integrity - critical analysis and update. *Cold Spring Harbor Perspectives in Biology*. 2013; *5*(5): 1–17.

28. Gredilla, R., Bohr, V. A., Stevnsner T. Mitochondrial DNA repair and association with aging - an update. Exp Gerontol. 2010; 45(7-8): 478–488.

29. Nickson, C. M., & Parsons, J. L. (2014). Monitoring regulation of DNA repair activities of cultured cells in-gel using the comet assay. *Frontiers in Genetics*, *5*(July), 1–11.

30. DiMauro S., Schon E. A. Mitochondrial Respiratory-Chain Diseases. *The new england journal of medicine*. 2003; 348(26): 2656-2668.

31. Tuppen, H. A. L., Blakely, E. L., Turnbull, D. M., Taylor, R. W. Mitochondrial DNA mutations and human disease. *Biochimica et Biophysica Acta*. 2010; *1797*(2): 113–128.

32. Rossignol, R., Faustin, B., Rocher, C., Malgat, M., Mazat, J. P., Letellier, T. Mitochondrial threshold effects. *The Biochemical Journal*. 2003; *370*: 751–762.

33. Dai, Y., Zheng, K., Clark, J., Swerdlow, R. H., Pulst, S. M., Sutton, J. P., Shinobu, L. A., Simon, D. K. Rapamycin drives selection against a pathogenic heteroplasmic mitochondrial DNA mutation. *Human Molecular Genetics*. 2014: *23*(3): 637–647.

34. Tanaka, M., Borgeld, H., Zhang, J., Muramatsu, S., Gong, J., Yoneda, M., Maruyama, W., Naoi M., Ibi, T., Sahashi, K., Shamoto, M., Fuku, N., Kurata, M., Yamada, Y., Nishizawa, K., Akao Y., Ohishi, N., Miyabayashi, S., Umemoto H., Muramatsu, T., Furukawa, K., Kikuchi A.,Nakano, I., Ozawa, K., Yagi, K. Gene Therapy for Mitochondrial Disease by Delivering Restriction Endonuclease Smal into Mitochondria. *Journal of Biomedical Science*. 2002; *9*: 534–41.

35. Minczuk, M., Papworth, M. a, Kolasinska, P., Murphy, M. P., & Klug, A. Sequence-specific modification of mitochondrial DNA using a chimeric zinc finger methylase. *Proceedings of the National Academy of Sciences of the United States of America*. 2006; *103*(52): 19689–19694.

36. Muratovska, A., Lightowlers, R. N., Taylor, R. W., Turnbull, D. M., Smith, R. a, Wilce, J. A, Martin, S. W., Murphy, M. P. Targeting peptide nucleic acid (PNA) oligomers to mitochondria within cells by conjugation to lipophilic cations: implications for mitochondrial DNA replication, expression and disease. *Nucleic Acids Research*. 2001; *29*(9) - 1852–1863.

37. Taivassalo, T., Haller, R. G.. Implications of exercise training in mtDNA defects--use it or lose it? *Biochimica et Biophysica Acta*. 2004; *1659*(2-3): 221–231.

38. Kyriakouli, D. S., Boesch, P., Taylor, R. W., & Lightowlers, R. N. Progress and prospects: gene therapy for mitochondrial DNA disease. *Gene Therapy*. 2008; *15*(14): 1017–1023.

39. Sato, M., Sato, K.. Maternal inheritance of mitochondrial DNA by diverse mechanisms to eliminate paternal mitochondrial DNA. *Biochimica et Biophysica Acta - Molecular Cell Research*. 2013; *1833*(8): 1979–1984.

40. De Paula, W. B. M., Agip, A. N. a, Missirlis, F., Ashworth, R., Vizcay-Barrena, G., Lucas, C. H., & Allen, J. F. Female and male gamete mitochondria are distinct and complementary in transcription, structure, and genome function. *Genome Biology and Evolution*. 2013; *5*(10): 1969–1977.

41. Samuels, D. C., Wonnapinij, P., Cree, L. M., & Chinnery, P. F. Reassessing evidence for a postnatal mitochondrial genetic bottleneck. *Nature Genetics*. 2010; *42*(6): 471–472.

42. Berg, J. M., Tymoczko, L. J., Stryer L. Biochemistry. 5th edition, 2002, New York.

43. Handy, D. E., & Loscalzo, J. Redox Regulation of Mitochondrial Function. *Antioxidants & Redox Signaling*. 2012; *16*(11): 1323–1367.

44. Turrens, J. F. Mitochondrial formation of reactive oxygen species. *The Journal of Physiology*. 2003; *552*: 335–344.

45. De Paula, W. B. M., Lucas, C. H., Agip, A.-N. A, Vizcay-Barrena, G., Allen, J. F. Energy, ageing, fidelity and sex: oocyte mitochondrial DNA as a protected genetic template. *Philosophical Transactions of the Royal Society of London. Series B, Biological Sciences*. 2013; 368(1622).

46. De Stefani, D., Patron, M., & Rizzuto, R. Structure and function of the mitochondrial calcium uniporter complex. *Biochimica et Biophysica Acta (BBA) - Molecular Cell Research*. 2015; 1853(9):2006-2011.

47. Williams, G. S. B., Boyman, L., Lederer, W. J. Mitochondrial calcium and the regulation of metabolism in the heart. *Journal of Molecular and Cellular Cardiology*. 2015; *78*: 35–45.

48. Brookes, P. S., Yoon, Y., Robotham, J. L., Anders, M. W., & Sheu, S. Calcium, ATP, and ROS : a mitochondrial love-hate triangle. *Am J Physiol Cell Physiol*. 2004, 287(4):C817-833.

49. Duchen, M. R., Verkhratsky, A., & Muallem, S.. Mitochondria and calcium in health and disease. *Cell Calcium*. 2008; *44*(1): 1–5.

50. Orrenius, S., Gogvadze, V., Zhivotovsky, B. Calcium and mitochondria in the regulation of cell death. *Biochemical and Biophysical Research Communications*. 2015;*460*(1): 72–81.

51. Ryu, S. Y., Beutner, G., Dirksen, R. T., Kinnally, K. W., Sheu, S. S. Mitochondrial ryanodine receptors and other mitochondrial Ca^{2+} permeable channels. *FEBS Letters*. 2010; *584*(10): 1948–1955.

52. Sifringer, M., Bendix, I., Börner, C., Endesfelder, S., von Haefen, C., Kalb, Holifanjaniaina S. , Prager, S. , Schlager, G. W., Keller, M., Jacotot, E., Felderhoff-Mueser, U. Prevention of neonatal oxygen-induced brain damage by reduction of intrinsic apoptosis. *Cell Death and Disease*. 2012; *3*(1): e250.

53. Chang, D. W., Xing, Z., Capacio, V. L., Peter, M. E., Yang, X. Interdimer processing mechanism of procaspase-8 activation. *EMBO Journal*. 2003; *22*(16): 4132–4142.

54. Favaloro, B., Allocati, N., Graziano, V., Di Ilio, C., De Laurenzi, V.. Role of apoptosis in disease. *Aging*. 2012; *4*(5): 330–349.

55. Fulda, S., Debatin, K. M. Extrinsic versus intrinsic apoptosis pathways in anticancer chemotherapy. *Oncogene*. 2006; *25*(34): 4798–4811.

56. Kroemer, G., Galluzzi, L., Brenner, C. Mitochondrial Membrane Permeabilization in Cell Death. *Physiology Reveiw*, 2007; 87(1):99-163.

57. Jonas, E. a., Porter, G. a., Beutner, G., Mnatsakanyan, N., Alavian, K. N. Cell death disguised: The mitochondrial permeability transition pore as the c-subunit of the F_1F_O ATP synthase. *Pharmacological Research*. 2015; 99:382-392.

58. Fulda, S. Targeting apoptosis for anticancer therapy. *Seminars in Cancer Biology*. 2014; *31*: 84–88.

59. Westermann, B. Bioenergetic role of mitochondrial fusion and fission. *Biochimica et Biophysica Acta – Bioenergetics*. 2012; *1817*(10): 1833–1838.

60. Hom, J., Sheu, S. S. Morphological dynamics of mitochondria - A special emphasis on cardiac muscle cells. *Journal of Molecular and Cellular Cardiology*. 2009; *46*(6): 811–820.

61. Mandemakers, W., Morais, V. a, De Strooper, B. A cell biological perspective on mitochondrial dysfunction in Parkinson disease and other neurodegenerative diseases. *Journal of Cell Science*. 2007; *120*: 1707–1716.

62. Ylikallio, E., Suomalainen, A. Mechanisms of mitochondrial diseases. *Annals of Medicine*. 2012; *44*(1): 41–59.

63. Wallace, D. C., Chalkia, D. Mitochondrial DNA genetics and the heteroplasmy conundrum in evolution and disease. *Cold Spring Harbor Perspectives in Biology*. 2013; 5(11):a021220.

64. Rossignol, R., Malgat, M., Mazat, J. P., Letellier, T. Threshold Effect and Tissue Specificity. *J of Biological Chemistry*. 1999; *274*: 33426–33432.

65. Schmiedel, J., Jackson, S., Schäfer, J., Reichmann, H. Mitochondrial cytopathies. *Journal of Neurology*. 2003; *250*(3): 267–277.

66. Chen, T., He, J., Huang, Y., Zhao, W. The generation of mitochondrial DNA large-scale deletions in human cells. *Journal of Human Genetics*. 2011; *56*(10): 689–694.

67. Szczepanowska, J., Malinska, D., Wieckowski, M. R., Duszynski, J. Effect of mtDNA point mutations on cellular bioenergetics. *Biochimica et Biophysica Acta – Bioenergetics*. 2012; *1817*(10): 1740–1746.

68. Kukat, A., Trifunovic, A. Somatic mtDNA mutations and aging - Facts and fancies. *Experimental Gerontology*. 2009; *44*(1-2): 101–105.

69. McFarland, R., Taylor, R. W., Turnbull, D. M. Mitochondrial Disease-Its Impact, Etiology, and Pathology. *Current Topics in Developmental Biology*. 2007; *77*(06): 113–155.

70. Chaturvedi, R. K., Beal, M. F. Mitochondria targeted therapeutic approaches in Parkinson's and Huntington's diseases. *Molecular and Cellular Neuroscience*. 2013; *55*: 101–114.

71. Dhillon, V. S., Fenech, M. Mutations that affect mitochondrial functions and their association with neurodegenerative diseases. *Mutation Research - Reviews in Mutation Research*. 2014; *759*(1): 1–13.

72. Corti, O., Lesage, S., Brice, a. What Genetics Tells us About the Causes and Mechanisms of Parkinson's Disease. *Physiological Reviews*. 2011; *91*(4): 1161–1218.

73. Gusdon, A. M., Fang, F., Chen, J., Mathews, C. E., Li, W., Chu, C. T., Chu, C. T., Ding, J., Chen, S. Association of the mt-ND2 5178A/C polymorphism with Parkinson's disease. *Neuroscience Letters*. 2015; *587*: 98–101.

74. Schapira, A. Mitochondrial dysfunction and oxidative stress in Parkinson's disease. *Neurochemical Research*.2011; *107*(3): 57–64.

75. De Rosa, P., Marini, E. S., Gelmetti, V., Valente, E. M. Candidate genes for Parkinson disease: Lessons from pathogenesis. *Clinica Chimica Acta*. 2015; 449:68-76

76. Kösel, S., Grasbon-Frodl, E. M., Mautsch, U., Egensperger, R., von Eitzen, U., Frishman, D., Hofman, S., Gerbitz, K., Mehraein, P., Graeber, M. B. Novel mutations of mitochondrial complex I in pathologically proven Parkinson disease. *Neurogenetics*. 1998; *1*(3): 197–204.

77. Finsterer, J. Parkinson's syndrome and Parkinson's disease in mitochondrial disorders. *Movement Disorders*. 2011; *26*(5): 784–791.

78. Andalib, S., Vafaee, M. S., & Gjedde, A. Parkinson's disease and mitochondrial gene variations: A review. *Journal of the Neurological Sciences*. 2014; *346*(1-2): 11–19.

79. McFarland, R., Taylor, R. W., Turnbull, D. M. A neurological perspective on mitochondrial disease. *The Lancet Neurology*. 2010; *9*(8): 829–840.

80. Zhao, D., Wang, C.-Q., Zhuo, R.-X., Cheng, S.-X. Modification of nanostructured calcium carbonate for efficient gene delivery. *Colloids and Surfaces. B, Biointerfaces*. 2014; *118*: 111–116.

81. Cwerman-Thibault, H., Sahel, J.-A., & Corral-Debrinski, M. Mitochondrial medicine: to a new era of gene therapy for mitochondrial DNA mutations. *Journal of Inherited Metabolic Disease*. 2011; *34*(2): 327–344.

82. Milane, L., Trivedi, M., Singh, A., Talekar, M., Amiji, M. Mitochondrial Biology, Targets, and Drug Delivery. *Journal of Controlled Release*. 2015; 207: 40–58

83. Abu-Salah, K. M., Ansari, A. A., Alrokayan, S. A. DNA-based applications in nanobiotechnology. *Journal of Biomedicine and Biotechnology*. 2010.

84. D'Souza, G. G. M., Boddapati, S. V., Weissig, V. Mitochondrial leader sequence-plasmid DNA conjugates delivered into mammalian cells by DQAsomes co-localize with mitochondria. *Mitochondrion*. 2005; *5*(5): 352–358.

85. Yoon, Y. G., Koob, M. D., Yoo, Y. H. Re-engineering the mitochondrial genomes in mammalian cells. *Anatomy & Cell Biology*. 2010; *43*(2): 97–109.

86. Yamada, Y., & Harashima, H. Mitochondrial drug delivery systems for macromolecule and their therapeutic application to mitochondrial diseases. *Advanced Drug Delivery Reviews*. 2008; *60*(13-14): 1439–1462.

87. Samal, S. K., Dash, M., Van Vlierberghe, S., Kaplan, D. L., Chiellini, E., van Blitterswijk, C., Moroni, L., Dubruel, P. Cationic polymers and their therapeutic potential. *Chemical Society Reviews*. 2012; *41*(21): 7147-7194.

88. Chen S., Li F., Zhuo R. and Cheng S. Efficient non-viral gene delivery mediated by nanostructured calcium carbonate in solution-based transfection and solid-phase transfection. *Mol. BioSyst*. 2011; 7: 2841–2847.

89. Costa, D., Valente, A., J., M., Miguel, M. G., Queiroz, J. Plasmid DNA microgels for drug/gene co-delivery: A promisingapproach for cancer therapy. *Colloids and Surfaces A: Physicochem. Eng. Aspects*. 2014; 442: 181– 190.